Copy 402
RM H55A10

NACA RM H55A10

NACA

RESEARCH MEMORANDUM

PRELIMINARY FLIGHT-DETERMINED PRESSURE DISTRIBUTIONS OVER THE WING OF THE DOUGLAS X-3 RESEARCH AIRPLANE AT SUBSONIC AND TRANSONIC MACH NUMBERS

By Gareth H. Jordan and C. Kenneth Hutchins, Jr.

High-Speed Flight Station
Edwards, Calif.

NATIONAL ADVISORY COMMITTEE
FOR AERONAUTICS

WASHINGTON

April 7, 1955

NACA RM H55A10 CONFIDENTIAL

NATIONAL ADVISORY COMMITTEE FOR AERONAUTICS

RESEARCH MEMORANDUM

PRELIMINARY FLIGHT-DETERMINED PRESSURE DISTRIBUTIONS OVER THE WING OF THE DOUGLAS X-3 RESEARCH AIRPLANE AT SUBSONIC AND TRANSONIC MACH NUMBERS

By Gareth H. Jordan and C. Kenneth Hutchins, Jr.

SUMMARY

Preliminary flight-measured chordwise pressure distributions have been obtained at a wing midsemispan station of the Douglas X-3 research airplane through an angle-of-attack range at Mach numbers of 0.61, 0.78, 0.94, and 1.10.

The results of the investigation indicate that the maximum section normal-force coefficient increased from about 0.7 at the lower Mach numbers to about 1.2 at a Mach number of 1.10. The pressure distributions at Mach numbers of about 0.61, 0.78, and 0.94 showed good agreement with wind-tunnel results. At Mach numbers of 0.94 and 1.10 leading-edge flap normal-force and hinge-moment coefficients increased with increase in angle of attack throughout the angle-of-attack range tested and resulted in high normal-force and hinge-moment coefficients at the higher angles of attack.

INTRODUCTION

The Douglas X-3 research airplane has completed the manufacturer's demonstration flights and U. S. Air Force evaluation flights at Edwards Air Force Base, Calif. NACA instrumentation was used during these flights to obtain limited measurements of the pressure distribution over a midsemispan station of the left wing prior to the flight test program to be conducted by the NACA High-Speed Flight Station.

Data were obtained during pull-ups at Mach numbers of approximately 0.61, 0.78, 0.94, and 1.10 at altitudes between 21,000 to 28,000 feet. The data were selected from the available maneuvers to cover as large a

range of angle of attack as possible and in each case maximum airplane normal-force coefficient was approached. This paper presents an analysis of the pressure distributions and section characteristics obtained during these preliminary flights.

SYMBOLS

$b/2$ wing semispan, ft

C_{N_A} airplane normal-force coefficient, nW/qS

c local wing section chord parallel to plane of symmetry, ft

c_f local leading-edge flap chord parallel to plane of symmetry, ft

c_h leading-edge flap section hinge-moment coefficient, $\int_0^1 (P_U - P_L)\left(\frac{x}{c_f} - 1\right)d\left(\frac{x}{c_f}\right)$

$c_{m_{c/4}}$ section pitching-moment coefficient about 0.25 local section chord point, $\int_0^1 (P_U - P_L)\left(\frac{x}{c} - \frac{1}{4}\right)d\left(\frac{x}{c}\right)$

c_n section normal-force coefficient, $\int_0^1 (P_L - P_U)d\left(\frac{x}{c}\right)$

c_{n_f} leading-edge flap section normal-force coefficient, $\int_0^1 (P_L - P_U)d\left(\frac{x}{c_f}\right)$

M free-stream Mach number

n airplane normal load factor, g units

P pressure coefficient, $\frac{p - p_o}{q}$

P_{vac} pressure coefficient when local pressure is a vacuum, $\frac{-1}{0.7M^2}$

p	local static pressure, lb/ft^2
p_o	free-stream static pressure, lb/ft^2
q	free-stream dynamic pressure, lb/ft^2
S	wing area, including area projected through fuselage, sq ft
t/c	airfoil thickness ratio, percent chord
W	airplane weight, lb
x	chordwise distance from leading edge of local section chord, ft
α	airplane angle of attack, deg

Subscripts:

L	lower surface
U	upper surface
cr	critical, the value for which the local flow first becomes sonic

DESCRIPTION OF AIRPLANE AND WING

The Douglas X-3 research airplane used in these tests and its general over-all dimensions are shown in the photograph and three-view drawing presented as figures 1 and 2, respectively. The dimensions and details of the wing are shown in figure 3. Physical characteristics of the airplane are given in table I and airfoil ordinates for the midsemispan station are given in table II.

The wing has an aspect ratio of 3.09, taper ratio of 0.39, a 4.5 percent thick modified hexagonal section and is mounted with zero incidence and dihedral. A line through the 75-percent local chords is perpendicular to the plane of symmetry. The modification to the airfoil section consisted of an 188-inch radius at 30 and 70 percent chord and leading- and trailing-edge radii as shown in table II.

INSTRUMENTATION AND DATA REDUCTION

Standard NACA instrumentation was used to measure the wing surface pressures, normal acceleration, control surface position, and angles of attack and sideslip. Indicated free-stream static and total pressures were measured on the nose boom from which Mach number and free-stream static pressure were obtained by the radar tracking method of reference 1.

The measured wing surface pressures were reduced to pressure coefficients and plotted to obtain chordwise pressure distributions which were mechanically integrated to obtain section normal-force coefficients and section pitching-moment coefficients. The section pressure distributions were also integrated over the leading-edge flap chord to obtain normal-force coefficients and hinge-moment coefficients of the leading-edge flap sections.

TESTS

The data presented were obtained from maneuvers made in the clean configuration through an angle-of-attack range at subsonic, transonic, and supersonic Mach numbers at altitudes between 21,000 and 28,000 feet. The Reynolds numbers for these tests based on wing mean aerodynamic chord, varied between 16×10^6 and 27×10^6.

ACCURACY

The accuracy of the test results is estimated to be within the following limits:

M	± 0.01
P	± 0.02
c_n	± 0.05
$c_{m_{c/4}}$	± 0.006
c_h	± 0.10

The angle-of-attack system was calibrated only under static ground conditions, hence the angle-of-attack data are subject to errors due to vane floating, boom and fuselage bending, and upwash. Pitching velocities were low for the points selected and the angles of attack have been corrected for the effective change in airstream direction.

RESULTS AND DISCUSSION

Pressure Distributions

Section pressure distributions obtained over the wing midsemispan station through an angle-of-attack range at approximately constant Mach numbers of 0.61, 0.78, 0.94, and 1.10 are presented in figures 4 to 7. These data are also shown in tabular form in tables III to VI.

Effect of angle of attack.- At a Mach number of 0.61 the pressures as shown in figure 4 were subcritical and resulted in a triangular chordwise loading at angles of attack from 8° to about 11°. At angles of attack of about 13° and greater extensive separation occurred over the upper surface.

At a Mach number of 0.78 (fig. 5) the pressures over the leading edge were supercritical with a shock located about 15-percent chord at an angle of attack of 5°. As the angle of attack increased the shock location became obscure probably as a result of separation. Essentially triangular chordwise loadings were obtained throughout the angle-of-attack range investigated at a Mach number of 0.78.

The pressure distributions at a Mach number of 0.94 (fig. 6) indicate high expansion around the leading edge and the presence of a shock near the leading edge. The main wing shock was located about 90-percent chord at an angle of attack of 3.4° and moved forward to about 45-percent chord as the angle of attack was increased to 8.4°.

The pressure distributions at a Mach number of about 1.10 (fig. 7) start near zero lift and indicate the progression of the high negative pressures over the leading edge. The expansion at the leading edge built up rapidly and moved rearward until at an angle of attack of about 10° the pressure near the leading edge closely approached a vacuum. A shock moved forward over the upper surface from the trailing edge to about 60-percent chord as the angle of attack increased from about 4° to 13°.

Effect of Mach number.- In figure 8 a comparison is shown of the pressure distributions obtained at an angle of attack of approximately 8° at the four test Mach numbers. At Mach numbers of 0.67 and 0.78 essentially triangular loading was obtained over the upper surface with a uniform pressure recovery to the trailing edge. At Mach numbers of 0.92 and 1.12 an expansion to a near vacuum state occurred around the leading edge. At a Mach number of 0.92 the main wing shock was located about 45-percent chord with separation behind the shock. At a Mach number of 1.12 a shock was located at about 90-percent chord.

Comparison with wind-tunnel results.- A comparison of the flight determined pressure distributions with wind-tunnel results (ref. 2) is

presented in figure 9. The pressure distributions showed good agreement with wind-tunnel results. The differences that occurred at Mach numbers greater than 0.90 (figs. 9(a) and 9(b)) are in the shock location and may be explained by small differences in Mach number. The difference that occurred in the pressure level over the forward 30-percent chord at a Mach number of 0.58 may be attributed to the difference in angle of attack. At this Mach number and angle of attack the flow over the upper surface is becoming completely separated and the difference in angle of attack could be responsible for the differences shown here (figs. 4(d) and 4(e)).

Section Aerodynamic Characteristics

The variation of airplane and section normal-force coefficient with angle of attack is shown in figure 10. At a Mach number of 0.61 the midsemispan station stalled at an angle of attack of about 11°; however, airplane normal-force coefficient continued to increase. The reduction in airplane normal-force-curve slope at an angle of attack of about 12° is probably associated with wing stall. The maximum normal-force coefficient of the midsemispan station increased from about 0.7 at the low Mach numbers to about 1.2 at a Mach number of 1.10.

The variation of section pitching-moment coefficient with normal-force coefficient is shown in figure 11. At Mach numbers of 0.61, 0.78, and 1.10 a stable variation of pitching moment occurred with an increase in stability at the higher normal-force coefficients. At a Mach number of 0.94 an unstable break occurred at a normal-force coefficient of about 0.60 and became stable again at a normal-force coefficient of about 0.70.

The variation of leading-edge flap normal-force coefficient and hinge-moment coefficient with angle of attack is shown in figures 12 and 13, respectively. At Mach numbers of 0.61 and 0.78 little variation of leading-edge flap loads occurred primarily because of the angle-of-attack range covered. At Mach numbers of 0.94 and 1.10 leading-edge flap normal-force and hinge-moment coefficients increased with increase in angle of attack throughout the angle-of-attack range tested and resulted in high normal-force and hinge-moment coefficients at the higher angles of attack.

CONCLUSIONS

Results of preliminary pressure-distribution measurements over a wing midsemispan station of the Douglas X-3 research airplane indicate that:

1. The maximum section normal-force coefficient increased from about 0.7 at the low Mach numbers to about 1.2 at a Mach number of 1.10.

2. The pressure distributions at Mach numbers of about 0.61, 0.78, and 0.94 showed good agreement with wind-tunnel results.

3. At Mach numbers of 0.94 and 1.10 leading-edge flap normal-force and hinge-moment coefficients increased with increase in angle of attack throughout the angle-of-attack range tested and resulted in high normal-force and hinge-moment coefficients at the higher angles of attack.

High-Speed Flight Station,
National Advisory Committee for Aeronautics,
Edwards, Calif., January 5, 1955.

REFERENCES

1. Zalovcik, John A.: A Radar Method of Calibrating Airspeed Installations on Airplanes in Maneuvers at High Altitudes and at Transonic and Supersonic Speeds. NACA Rep. 985, 1950. (Supersedes NACA TN 1979.)

2. Cleary, Joseph W., and Mellenthin, Jack A.: Wind-Tunnel Tests of a 0.16-Scale Model of the X-3 Airplane at High Subsonic Speeds. Wing and Fuselage Pressure Distribution. NACA RM A50D07, 1950.

TABLE I

PHYSICAL CHARACTERISTICS OF THE DOUGLAS

X-3 RESEARCH AIRPLANE

Wing:	
Area, sq ft	166.5
Span, ft	22.69
Aspect ratio	3.09
Taper ratio	0.39
Airfoil section	Modified hexagon
Airfoil thickness ratio, percent chord	4.5
Airfoil leading- and trailing-edge angles, deg	8.58
Mean aerodynamic chord, ft	7.84
Root chord, ft	10.58
Tip chord, ft	4.11
Sweep at leading edge, deg	23.16
Sweep at 0.75 chord line, deg	0
Sweep at trailing edge, deg	-8.12
Incidence, deg	0
Dihedral, deg	0
Geometric twist, deg	0
Horizontal tail:	
Area, sq ft	43.24
Span, ft	13.77
Aspect ratio	4.38
Taper ratio	0.405
Airfoil section	Modified hexagon
Airfoil thickness ratio at root chord, percent chord	8.01
Airfoil thickness ratio outboard of station 26, percent chord	4.5
Mean aerodynamic chord, ft	3.34
Root chord, ft	4.475
Tip chord, ft	1.814
Sweep at trailing edge, deg	0
Dihedral, deg	0
Vertical tail:	
Area, sq ft	23.73
Span, ft	5.59
Aspect ratio	1.315
Taper ratio	0.292
Airfoil section	Modified hexagon
Airfoil thickness ratio, percent chord	4.5
Mean aerodynamic chord, ft	4.69
Root chord, ft	6.508
Tip chord, ft	1.93
Sweep at leading edge, deg	45.00
Fuselage:	
Length, including boom, ft	66.75
Maximum width, ft	6.08
Maximum height, ft	4.81
Power plant:	
Engines	Two J34-WE-17 with afterburner
Rating, each engine:	
Static sea-level military thrust, lb	3,370
Static sea-level maximum thrust, lb	4,850
Weight:	
Basic (without fuel, oil, water, pilot), lb	16,120
Total	22,100

TABLE II

PROFILE AND ORDINATES OF THE WING SECTION AT STATION 0.625 b/2

[Modified 4.5-percent-thick hexagonal airfoil]

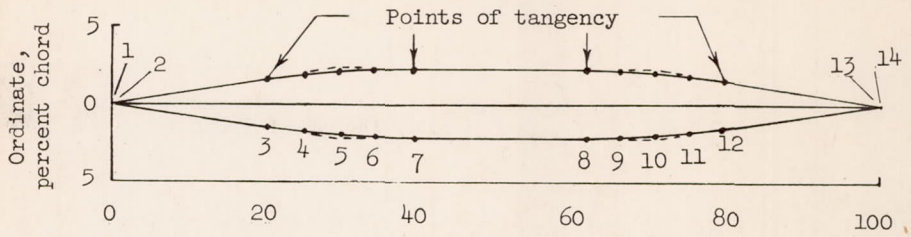

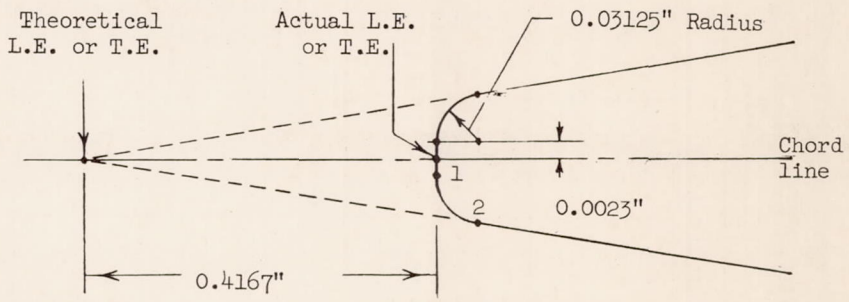

DIMENSIONS OF L.E. AND T.E.
(Same at all stations)

[Stations and ordinates given in percent of local chord]

Station number	Upper surface		Lower surface	
	Station	Ordinate	Station	Ordinate
1	0	0.003	0	-0.003
2	.037	.042	.037	-.042
3	19.948	1.536	19.948	-1.536
4	24.709	1.848	24.709	-1.848
5	29.477	2.072	29.477	-2.072
6	34.248	2.206	34.248	-2.206
7	39.023	2.250	39.023	-2.250
8	61.558	2.250	61.558	-2.250
9	66.043	2.208	66.043	-2.208
10	70.526	2.082	70.526	-2.082
11	75.005	1.872	75.005	-1.872
12	79.480	1.579	79.480	-1.579
13	99.963	.042	99.963	-.042
14	100.000	.003	100.000	-.003

TABLE III

PRESSURE COEFFICIENTS AT MIDSEMISPAN STATION

[X-3 airplane; M ≈ 0.61]

x/c	Upper surface											
2.5	-0.876	-0.814	-0.868	-0.831	-0.532	-0.440	-0.369	-0.429	-0.409	-0.463	-0.432	-0.442
5.0	-.851	-.832	-.871	-.853	-.562	-.436	-.383	-.443	-.386	-.496	-.521	-.438
7.5	-.868	-.893	-.860	-.908	-.609	-.486	-.451	-.456	-.491	-.546	-.572	-.434
10.1	-.810	-.890	-.900	-.870	-.580	-.492	-.401	-.480	-.423	-.607	-.502	-.438
18.0	-.830	-.882	-.835	-.849	-.638	-.536	-.482	-.469	-.487	-.595	-.529	-.466
20.3	-.876	-.872	-.808	-.864	-.642	-.593	-.481	-.485	-.464	-.595	-.565	-.538
29.5	-.760	-.706	-.804	-.825	-.668	-.599	-.524	-.510	-.526	-.601	-.551	-.544
36.0	-.594	-.566	-.699	-.745	-.631	-.548	-.512	-.553	-.535	-.572	-.542	-.534
47.5	-.518	-.498	-.565	-.710	-.609	-.575	-.538	-.581	-.674	-.673	-.603	-.576
55.0	-.399	-.362	-.395	-.549	-.567	-.536	-.607	-.595	-.630	-.559	-.547	-.540
68.8	-.229	-.213	-.244	-.318	-.526	-.586	-.549	-.535	-.533	-.645	-.615	-.608
80.0	-.116	-.194	-.182	-.248	-.479	-.499	-.518	-.613	-.558	-.595	-.621	-.614
98.0	-.062	-.081	-.139	-.138	-.373	-.352	-.518	-.613	-.612	-.632	-.621	-.651
x/c	Lower surface											
2.5	0.645	0.682	0.774	0.691	0.763	0.792	0.710	0.742	0.705	0.734	0.794	0.776
5.0	.525	.558	.622	.630	.712	.665	.675	.671	.616	.665	.725	.742
7.5	.504	.479	.542	.557	.649	.580	.647	.662	.644	.582	.642	.677
10.1	.364	.377	.410	.426	.432	.393	.551	.511	.546	.484	.524	.576
17.9	.249	.270	.301	.274	.332	.307	.361	.339	.302	.383	.404	.455
24.5	.214	.191	.221	.249	.270	.298	.292	.330	.276	.340	.323	.337
38.0	.060	.087	.145	.115	.103	.106	.128	.177	.051	.075	.166	.234
55.0	-.021	.003	.061	.037	.033	-.041	-.051	-.038	.053	-.069	-.109	-.023
74.1	-.049	-.055	.003	-.092	-.092	-.078	-.089	-.224	-.129	-.256	-.204	-.155
90.0	-.063	-.026	-.011	-.075	-.146	-.191	-.162	-.277	-.221	-.385	-.240	-.230
98.0	.006	-.039	-.026	-.090	-.356	-.334	-.320	-.487	-.576	-.559	-.547	-.632
α	8.2°	8.3°	9.3°	10.3°	12.7°	13.6°	14.2°	15.7°	17.0°	18.2°	18.7°	19.4°
c_n	0.57	0.58	0.66	0.68	0.66	0.61	0.61	0.62	0.61	0.62	0.63	0.65
$c_{m_{c/4}}$	-0.0122	-0.0202	-0.0368	-0.0400	-0.0755	-0.0730	-0.0899	-0.0787	-0.0883	-0.0627	-0.0536	-0.0857
M	0.67	0.66	0.65	0.62	0.58	0.57	0.56	0.56	0.56	0.56	0.55	0.55

TABLE IV

PRESSURE COEFFICIENTS AT MIDSEMISPAN STATION

[X-3 airplane; M ≈ 0.78]

x/c	Upper surface							
2.5	-1.161	-1.004	-1.070	-1.079	-0.922	-0.915	-0.918	-0.902
5.0	-1.095	-1.008	-1.051	-1.073	-.943	-.950	-.946	-.923
7.5	-1.031	-1.012	-1.018	-1.093	-.956	-1.032	-.974	-.966
10.1	-.848	-1.000	-.997	-1.081	-.952	-.982	-1.002	-.939
18.0	-.495	-.768	-.856	-.915	-.887	-.895	-.789	-.830
20.3	-.420	-.694	-.751	-.833	-.830	-.826	-.714	-.774
29.5	-.330	-.477	-.535	-.605	-.681	-.707	-.683	-.712
36.0	-.284	-.357	-.387	-.444	-.566	-.601	-.686	-.652
47.5	-.214	-.266	-.290	-.331	-.474	-.509	-.660	-.589
55.0	-.171	-.187	-.235	-.215	-.356	-.369	-.586	-.506
68.8	-.151	-.150	-.164	-.129	-.225	-.260	-.368	-.440
80.0	-.047	-.080	-.086	-.062	-.058	-.152	-.257	-.305
98.0	.119	.092	.055	.062	-.042	-.052	-.108	-.143
x/c	Lower surface							
2.5	0.560	0.568	0.570	0.641	0.690	0.698	0.721	0.721
5.0	.448	.456	.476	.575	.576	.582	.628	.638
7.5	.368	.377	.405	.448	.493	.455	.499	.513
10.1	.282	.265	.300	.343	.396	.370	.442	.431
17.9	.185	.177	.188	.225	.264	.305	.330	.321
24.5	.088	.096	.125	.164	.187	.185	.250	.226
38.0	.020	.028	.022	.095	.087	.095	.111	.135
55.0	-.006	.011	-.007	.049	.055	.042	.041	.051
74.1	-.075	-.100	-.106	-.080	-.061	-.102	-.104	-.125
90.0	.020	.003	.006	-.012	.006	-.045	-.047	-.083
98.0	.152	.119	.105	.119	.038	.041	-.022	-.058
α	5.0°	5.3°	5.8°	6.3°	7.1°	7.2°	8.8°	9.2°
c_n	0.37	0.44	0.46	0.52	0.57	0.60	0.68	0.67
$c_{m_{c/4}}$	0.0214	0.0198	0.0173	0.0163	-0.0054	-0.0118	-0.0400	-0.0368
M	0.77	0.77	0.77	0.77	0.78	0.78	0.78	0.78

TABLE V

PRESSURE COEFFICIENTS AT MIDSEMISPAN STATION

[X-3 airplane; M ≈ 0.94]

x/c	Upper surface									
2.5	-0.919	-0.967	-0.998	-1.042	-1.096	-1.138	-1.249	-1.263	-1.349	-1.383
5.0	-.793	-.794	-.865	-.901	-.941	-.990	-1.084	-1.132	-1.192	-1.262
7.5	-.677	-.738	-.769	-.824	-.877	-.925	-1.024	-1.058	-1.153	-1.179
10.1	-.604	-.659	-.703	-.753	-.827	-.875	-.975	-1.009	-1.132	-1.172
18.0	-.170	-.354	-.602	-.637	-.716	-.743	-.846	-.833	-.937	-.975
20.3	-.202	-.284	-.439	-.605	-.687	-.722	-.835	-1870	-.977	-1.010
29.5	-.390	-.397	-.417	-.474	-.626	-.772	-.901	-.929	-.997	-1.080
36.0	-.493	-.500	-.486	-.533	-.578	-.618	-.790	-.895	-.999	-1.064
47.5	-.534	-.577	-.575	-.600	-.635	-.664	-.745	-.781	-.972	-.705
55.0	-.492	-.519	-.530	-.565	-.605	-.638	-.700	-.726	-.815	-.595
68.8	-.490	-.564	-.582	-.585	-.659	-.646	-.716	-.716	-.502	-.554
80.0	-.552	-.585	-.628	-.605	-.624	-.665	-.381	-.301	-.431	-.528
98.0	.080	.047	.047	.032	.024	-.001	-.069	-.115	-.262	-.379
x/c	Lower surface									
2.5	0.461	0.520	0.538	0.575	0.594	0.608	0.640	0.673	0.680	0.722
5.0	.334	.382	.400	.445	.451	.492	.510	.537	.649	.585
7.5	.286	.293	.332	.398	.384	.411	.422	.470	.508	.509
10.1	.201	.227	.227	.309	.289	.329	.338	.358	.360	.381
17.9	.106	.119	.165	.176	.182	.209	.230	.257	.284	.326
24.5	-.025	.023	.057	.048	.068	.081	.136	.136	.196	.190
38.0	-.164	-.124	-.110	-.086	-.060	-.008	-.002	.031	.048	.075
55.0	-.092	-.058	-.038	-.033	-.040	-.021	-.008	.005	-.025	.008
74.1	-.324	-.338	-.337	-.292	-.333	-.320	-.311	-.297	-.284	-.307
90.0	-.402	-.395	-.394	-.343	-.370	-.350	-.348	-.335	-.357	-.338
98.0	-.177	-.203	-.222	-.217	-.250	-.244	-.288	-.295	-.390	-.392
α	3.4°	3.6°	4.0°	4.4°	4.9°	5.3°	6.2°	6.3°	7.3°	8.4°
c_n	0.33	0.40	0.45	0.51	0.56	0.62	0.66	0.69	0.80	0.80
$c_{m_{c/4}}$	-0.0045	-0.0170	-0.0205	-0.0288	-0.0230	-0.0336	-0.0115	-0.0109	-0.0291	-0.0368
M	0.94	0.94	0.94	0.94	0.94	0.94	0.93	0.93	0.92	0.92

TABLE VI

PRESSURE COEFFICIENTS AT MIDSEMISPAN STATION

[X-3 airplane; M ≈ 1.10]

x/c	Upper surface						
2.5	0.258	-0.168	-0.423	-0.472	-0.526	-0.619	-0.682
5.0	.236	.198	-.249	-.340	-.376	-.469	-.549
7.5	.197	.155	-.051	-.270	-.340	-.437	-.516
10.1	.165	.136	.012	-.234	-.294	-.387	-.495
18.0	.142	.141	.109	-.003	-.207	-.315	-.399
20.3	-.094	-.105	-.120	-.148	-.186	-.290	-.462
29.5	.097	.052	.053	-.004	-.146	-.314	-.390
36.0	-.213	-.212	-.226	-.260	-.290	-.328	-.395
47.5	-.182	-.202	-.253	-.290	-.313	-.342	-.416
55.0	-.197	-.214	-.250	-.268	-.315	-.358	-.404
68.8	-.241	-.246	-.260	-.329	-.365	-.404	-.457
80.0	-.295	-.309	-.338	-.376	-.401	-.438	-.484
98.0	-.347	-.336	-.332	-.306	-.299	-.278	-.309
x/c	Lower surface						
2.5	0.423	0.474	0.516	0.569	0.629	0.669	0.718
5.0	.273	.324	.380	.448	.500	.541	.588
7.5	.189	.238	.312	.393	.424	.467	.520
10.1	.151	.166	.238	.274	.316	.379	.405
17.9	.125	.164	.198	.241	.272	.294	.347
24.5	.048	.067	.114	.143	.165	.204	.227
38.0	-.157	-.125	-.095	-.057	-.013	.021	.056
55.0	-.117	-.064	-.006	.009	.063	.150	.181
74.1	-.243	-.214	-.182	-.135	-.146	-.120	-.110
90.0	-.312	-.298	-.283	-.251	-.261	-.229	-.218
98.0	-.312	-.292	-.288	-.273	-.266	-.240	-.240
α	1.5°	1.8°	2.6°	3.3°	3.6°	4.6°	5.7°
c_n	0.05	0.10	0.19	0.28	0.35	0.46	0.55
$c_{m_{c/4}}$	-0.0128	-0.0147	-0.0182	-0.0234	-0.0333	-0.0464	-0.0598
M	1.09	1.10	1.10	1.11	1.11	1.11	1.11

TABLE VI.- Concluded

PRESSURE COEFFICIENTS AT MIDSEMISPAN STATION

[X-3 airplane; M ≈ 1.10]

x/c	Upper surface					
2.5	-0.781	-0.826	-1.010	-1.049	-1.104	-1.122
5.0	-.629	-.650	-.857	-.916	-1.027	-1.024
7.5	-.616	-.651	-.836	-.899	-.972	-.990
10.1	-.597	-.638	-.805	-.890	-.947	-.972
18.0	-.496	-.522	-.704	-.776	-.857	-.900
20.3	-.525	-.580	-.768	-.834	-.800	-.913
29.5	-.518	-.557	-.727	-.781	-.824	-.852
36.0	-.546	-.616	-.775	-.862	-.881	-.906
47.5	-.477	-.606	-.844	-.896	-.965	-.967
55.0	-.460	-.492	-.770	-.832	-.888	-.890
68.8	-.497	-.529	-.742	-.843	-.656	-.658
80.0	-.527	-.562	-.729	-.771	-.643	-.671
98.0	-.315	-.278	-.340	-.411	-.526	-.539
x/c	Lower surface					
2.5	0.749	0.817	0.939	0.969	0.973	0.977
5.0	.618	.680	.825	.880	.889	.882
7.5	.552	.621	.721	.777	.826	.788
10.1	.443	.482	.625	.649	.697	.690
17.9	.387	.447	.557	.589	.629	.617
24.5	.277	.335	.473	.502	.550	.537
38.0	.160	.239	.355	.399	.430	.413
55.0	.205	.207	.278	.311	.332	.340
74.1	-.100	-.077	-.014	.024	.049	.031
90.0	-.211	-.170	-.117	-.064	-.025	-.048
98.0	-.222	-.172	-.109	-.072	-.058	-.060
α	6.8°	7.4°	10.6°	11.8°	13.1°	13.4°
c_n	0.64	0.73	1.02	1.13	1.15	1.15
$c_{m_{c/4}}$	-0.0746	-0.0886	-0.1453	-0.1741	-0.1632	-0.1645
M	1.12	1.12	1.11	1.11	1.10	1.10

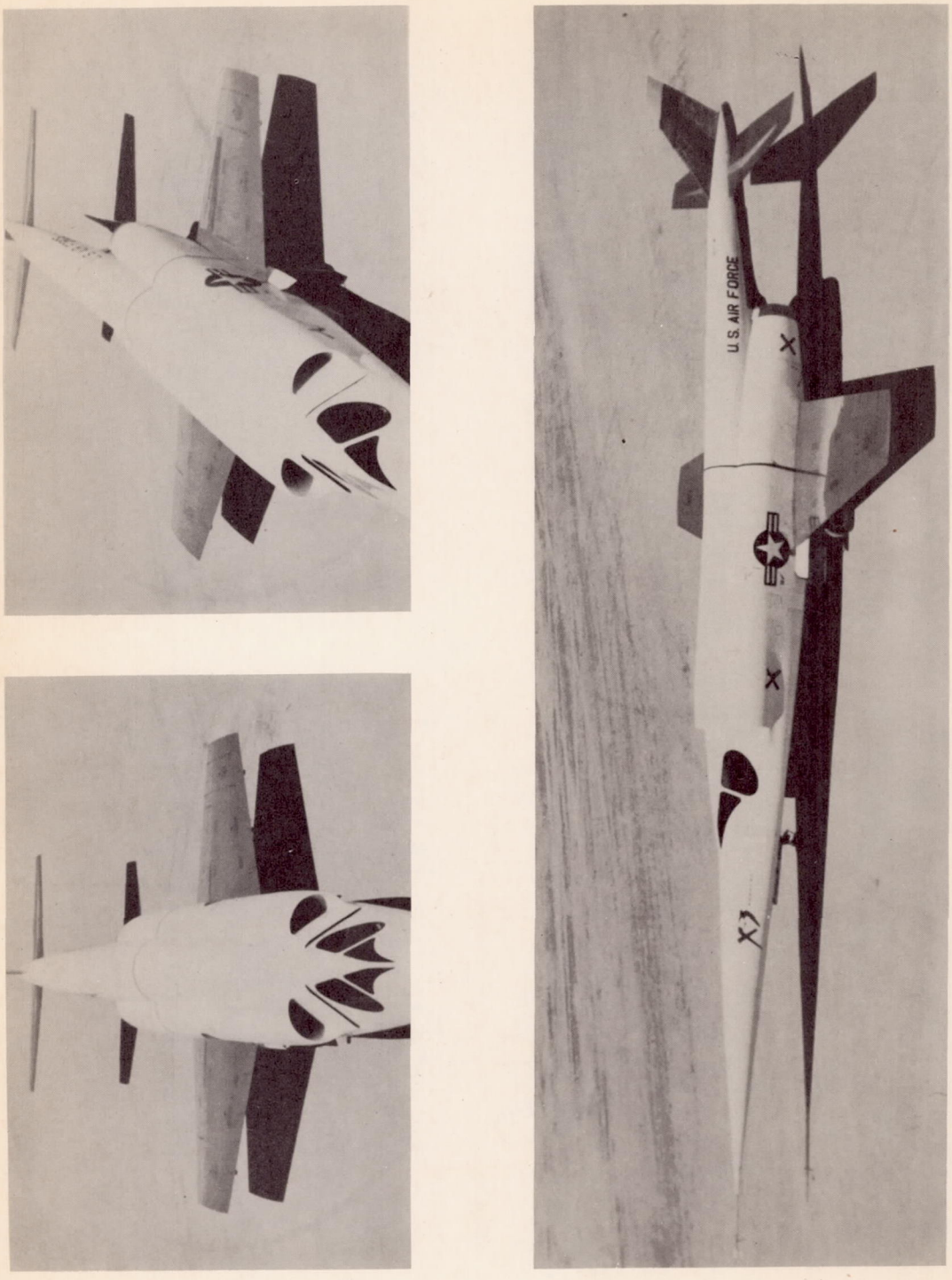

L-87503

Figure 1.- Photographs of Douglas X-3 research airplane.

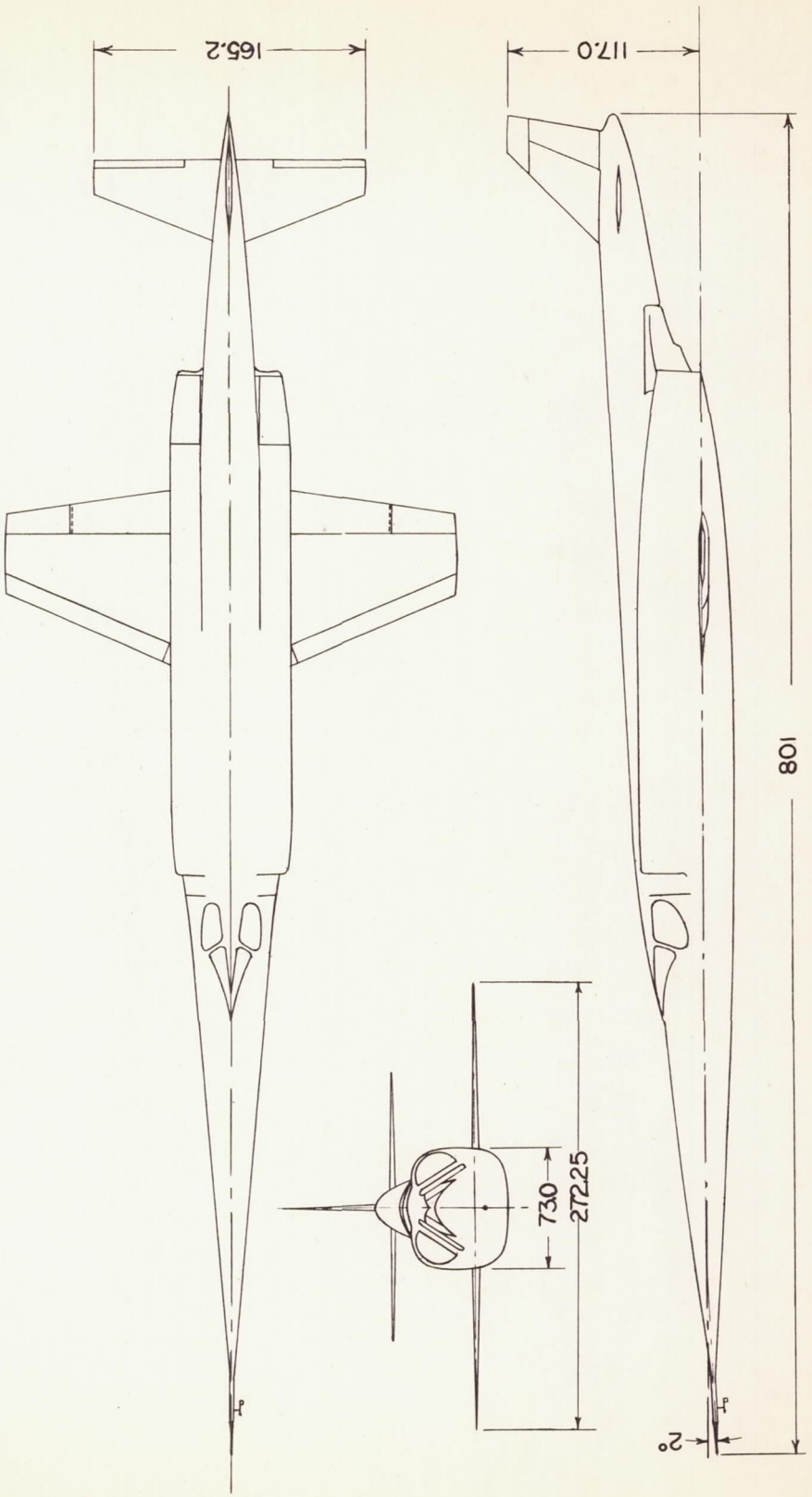

Figure 2.- Three-view drawing of the X-3 airplane. All dimensions are in inches.

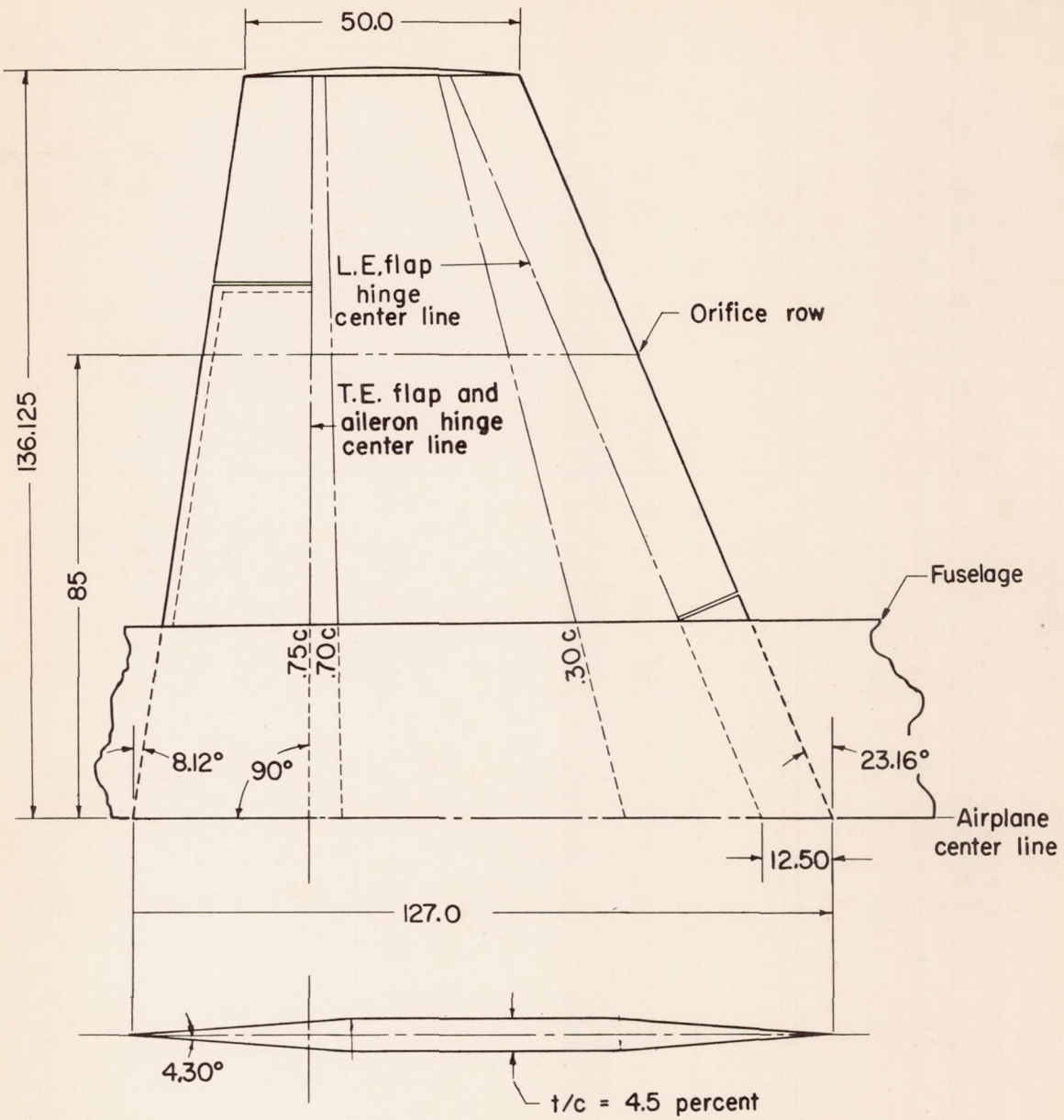

Figure 3.- Drawing of the X-3 left wing including spanwise location of the pressure-measuring orifice row. All dimensions in inches unless otherwise stated.

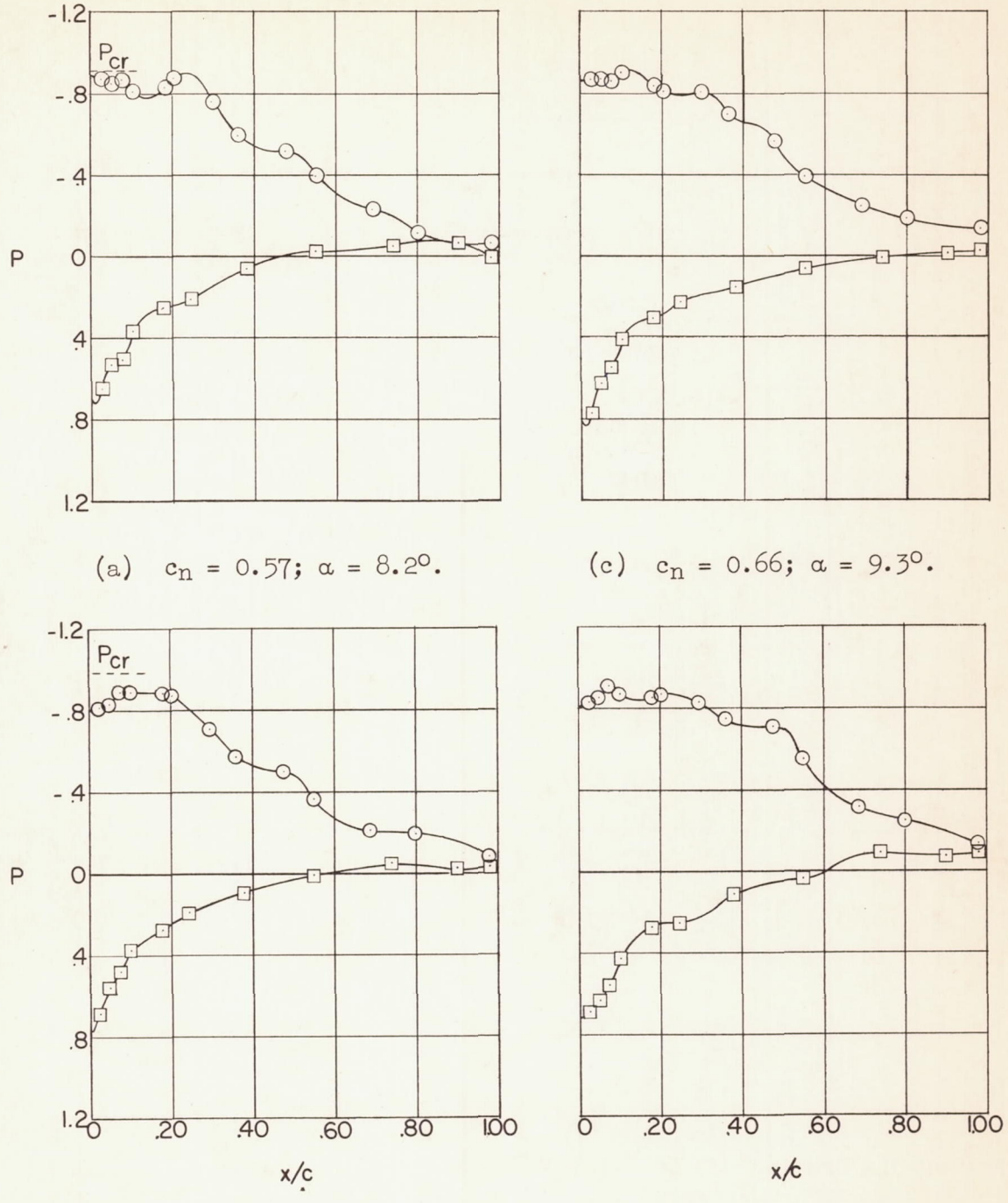

(a) $c_n = 0.57$; $\alpha = 8.2^\circ$.

(c) $c_n = 0.66$; $\alpha = 9.3^\circ$.

(b) $c_n = 0.58$; $\alpha = 8.3^\circ$.

(d) $c_n = 0.68$; $\alpha = 10.3^\circ$.

Figure 4.- Effects of angle of attack on the chordwise pressure distribution of the midsemispan station. M = 0.61 ± 0.06. X-3 airplane.

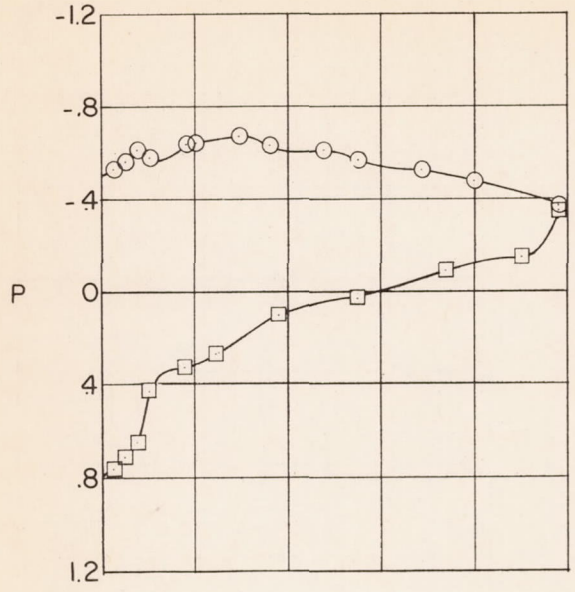

(e) $c_n = 0.66$; $\alpha = 12.7^\circ$.

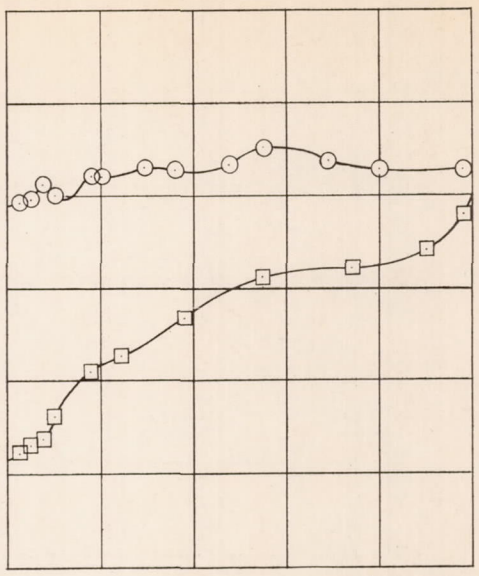

(g) $c_n = 0.61$; $\alpha = 14.2^\circ$.

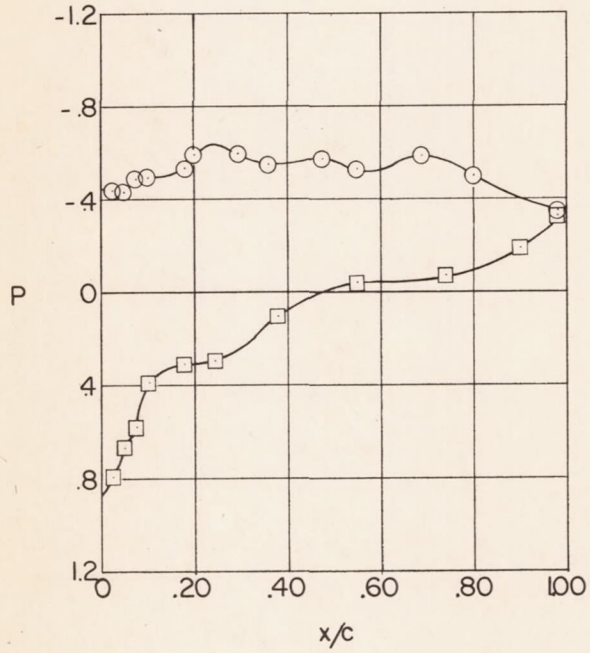

(f) $c_n = 0.61$; $\alpha = 13.6^\circ$.

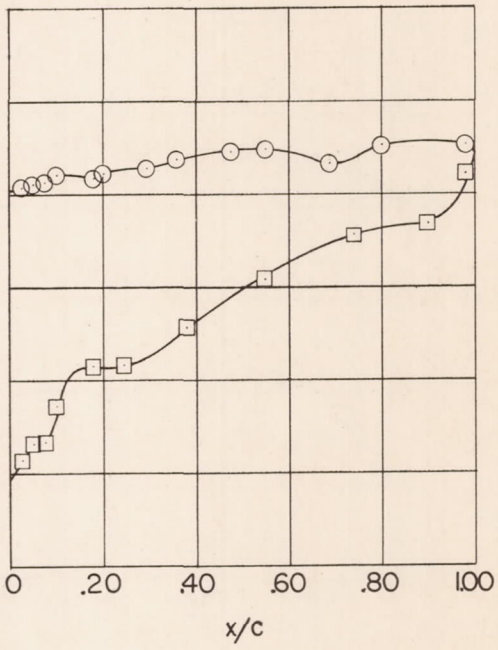

(h) $c_n = 0.62$; $\alpha = 15.7^\circ$.

Figure 4.- Continued.

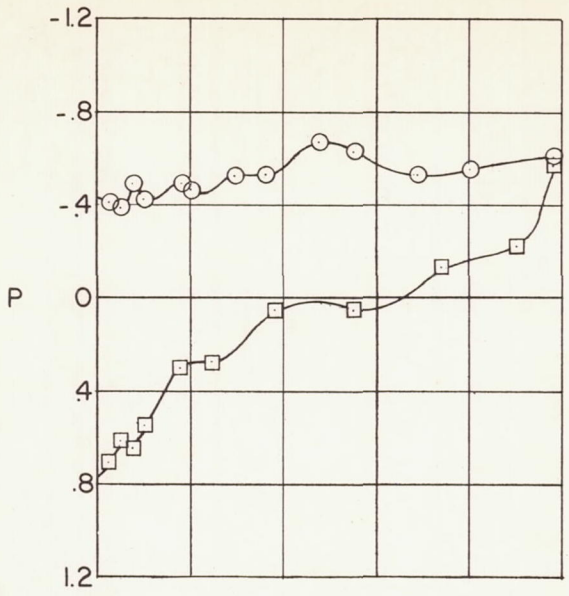

(i) $c_n = 0.61$; $\alpha = 17.0^\circ$.

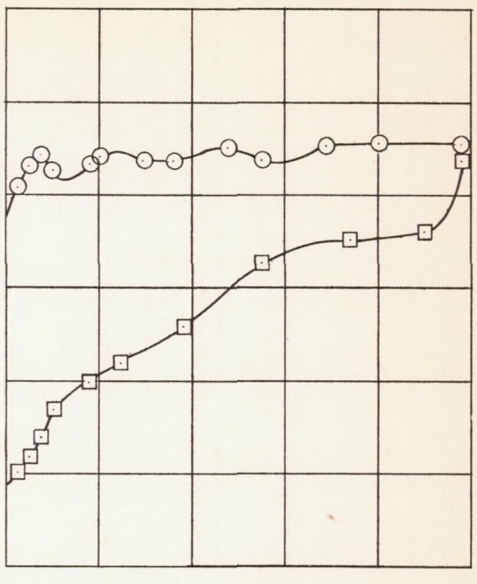

(k) $c_n = 0.63$; $\alpha = 18.7^\circ$.

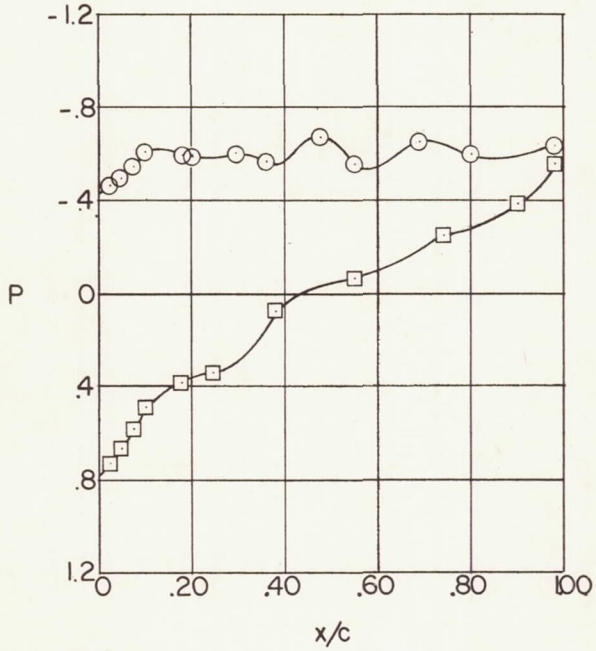

(j) $c_n = 0.62$; $\alpha = 18.2^\circ$.

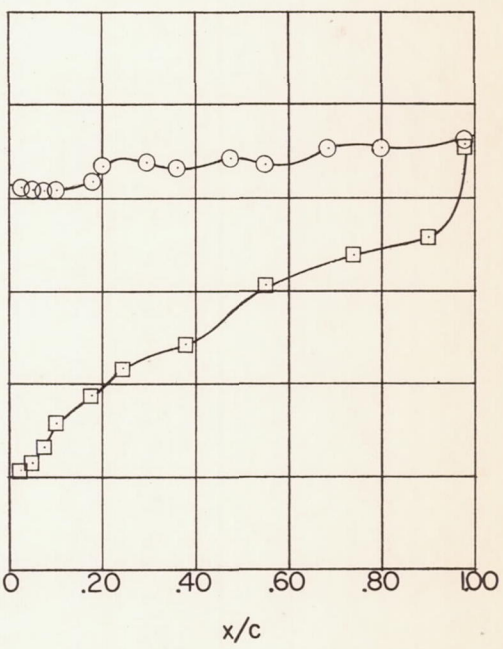

(l) $c_n = 0.65$; $\alpha = 19.4^\circ$.

Figure 4.- Concluded.

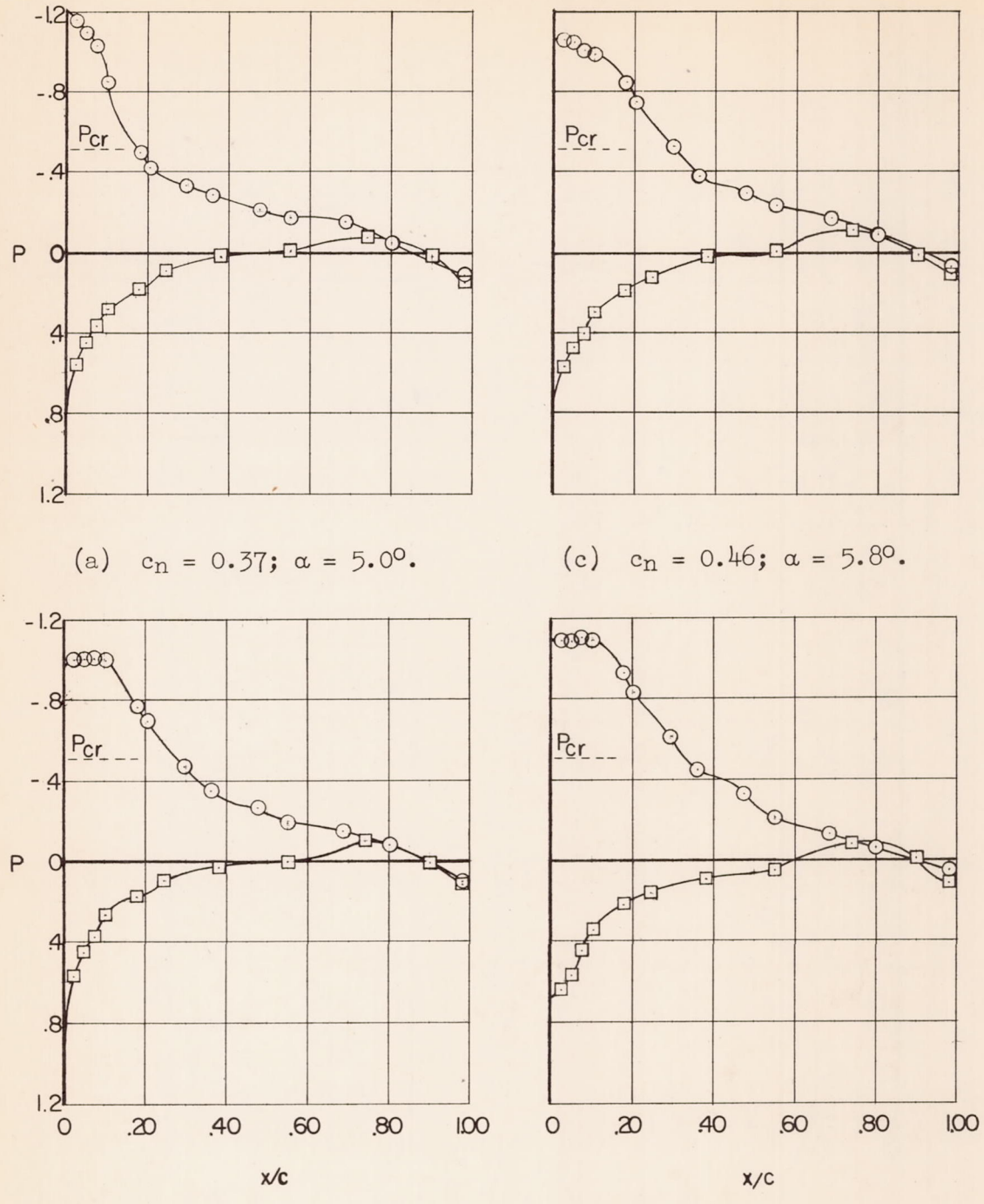

(a) $c_n = 0.37$; $\alpha = 5.0^\circ$.

(c) $c_n = 0.46$; $\alpha = 5.8^\circ$.

(b) $c_n = 0.44$; $\alpha = 5.3^\circ$.

(d) $c_n = 0.52$; $\alpha = 6.3^\circ$.

Figure 5.- Effects of angle of attack on the chordwise pressure distribution of the midsemispan station. M = 0.78 ± 0.01. X-3 airplane.

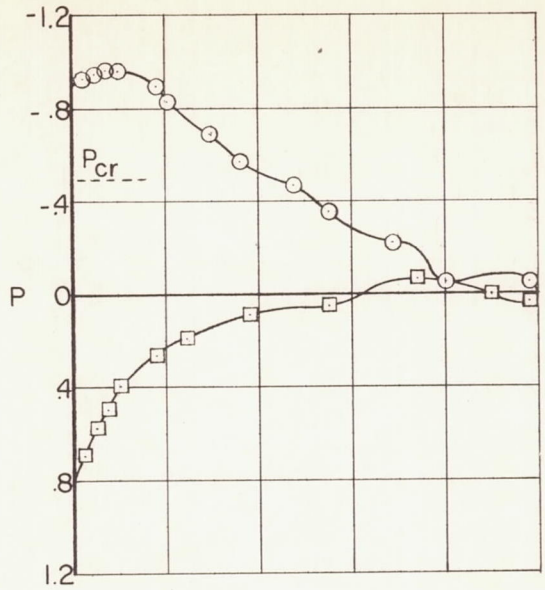

(e) $c_n = 0.57$; $\alpha = 7.1^\circ$.

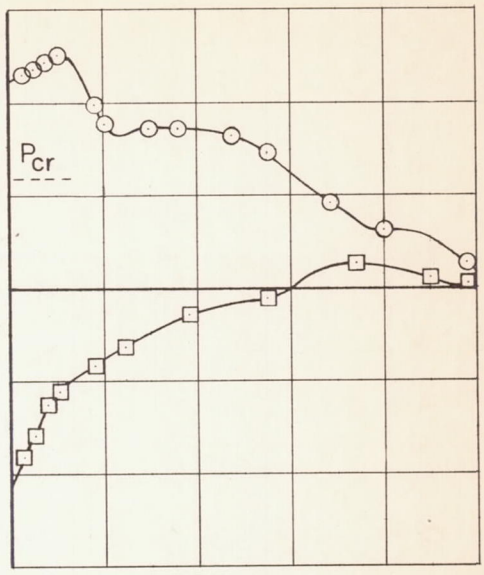

(g) $c_n = 0.68$; $\alpha = 8.8^\circ$.

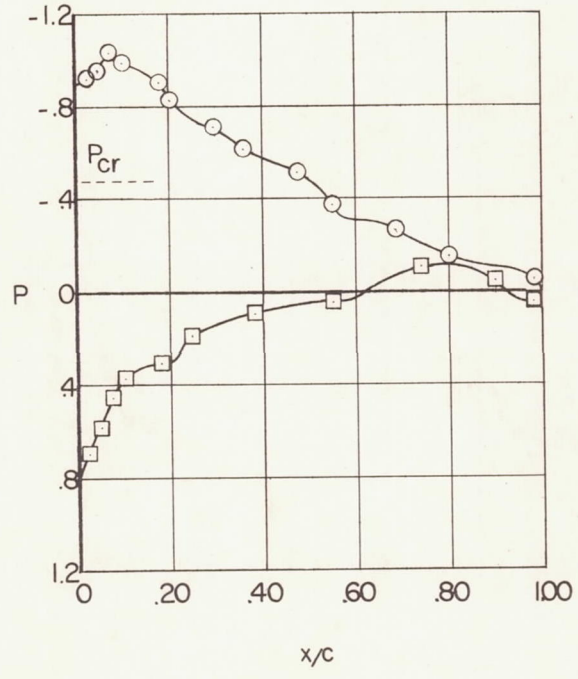

(f) $c_n = 0.60$; $\alpha = 7.2^\circ$.

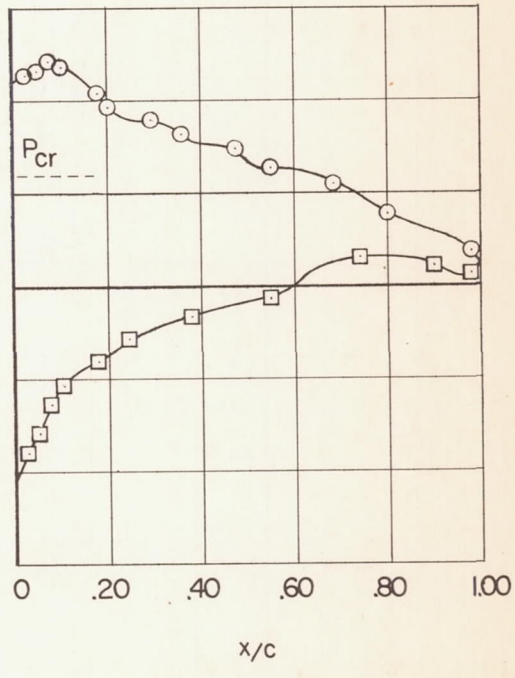

(h) $c_n = 0.67$; $\alpha = 9.2^\circ$.

Figure 5.- Concluded.

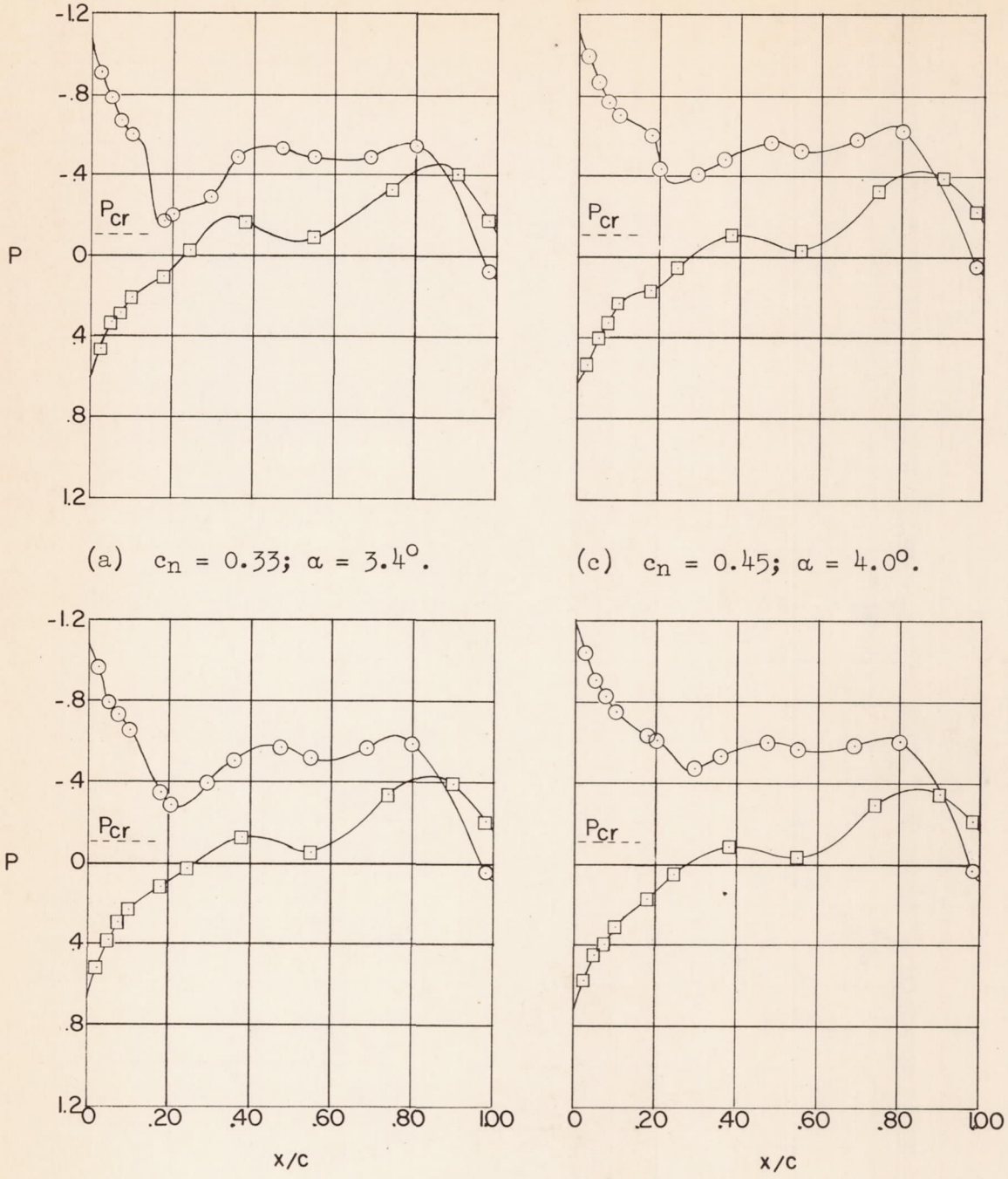

(a) $c_n = 0.33$; $\alpha = 3.4^\circ$.

(c) $c_n = 0.45$; $\alpha = 4.0^\circ$.

(b) $c_n = 0.40$; $\alpha = 3.6^\circ$.

(d) $c_n = 0.51$; $\alpha = 4.4^\circ$.

Figure 6.- Effects of angle of attack on the chordwise pressure distribution of the midsemispan station at a Mach number of 0.94 ± 0.02. X-3 airplane.

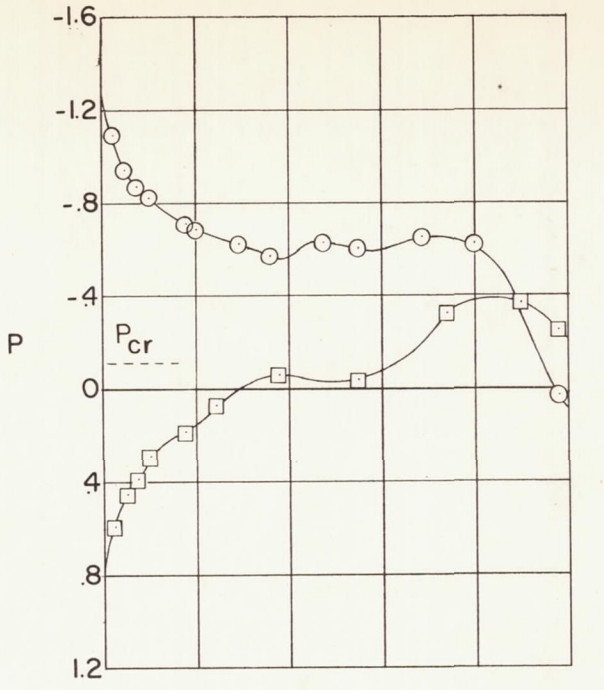

(e) $c_n = 0.56$; $\alpha = 4.9^\circ$.

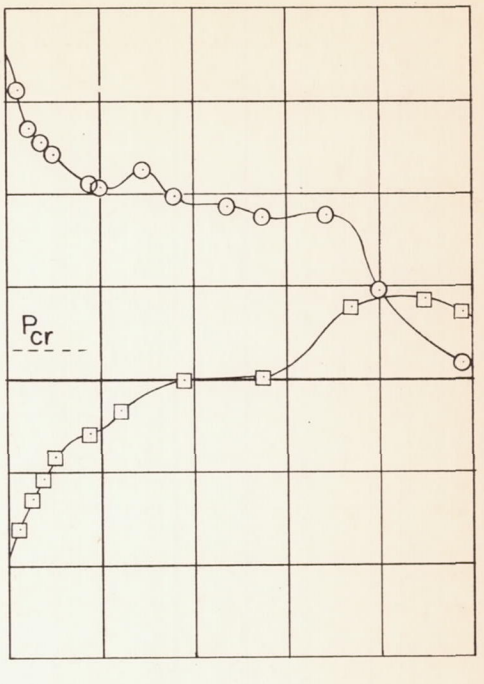

(g) $c_n = 0.66$; $\alpha = 6.2^\circ$.

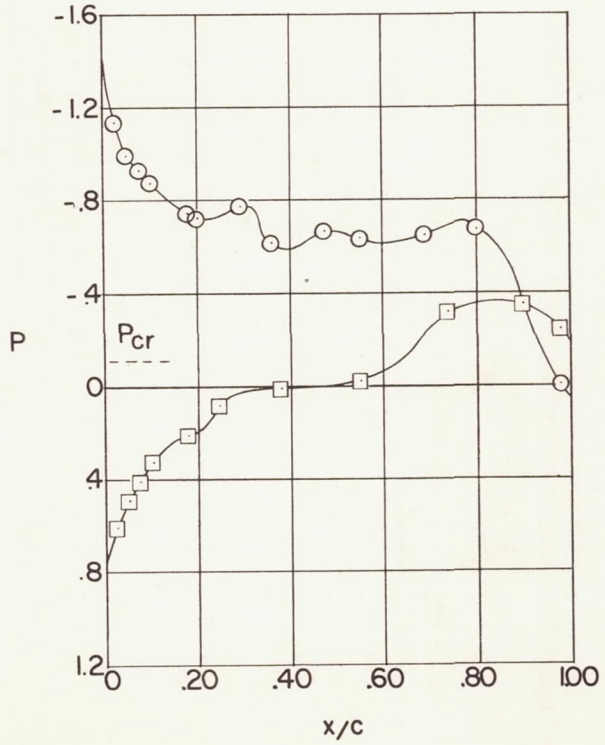

(f) $c_n = 0.62$; $\alpha = 5.3^\circ$.

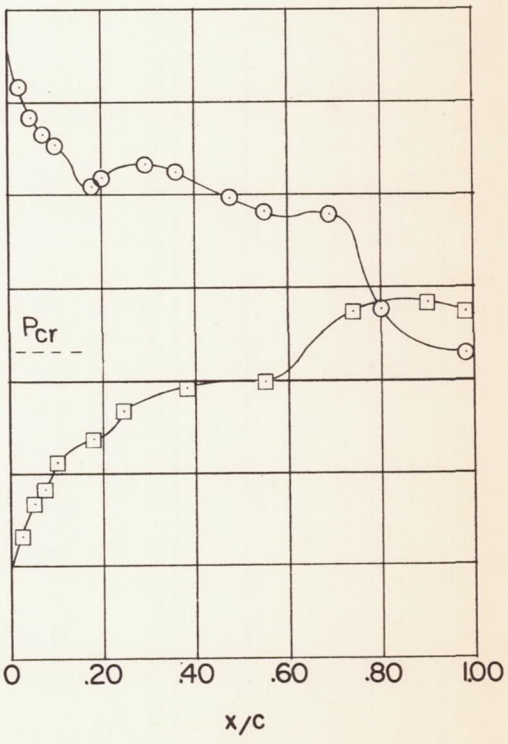

(h) $c_n = 0.69$; $\alpha = 6.3^\circ$.

Figure 6.- Continued.

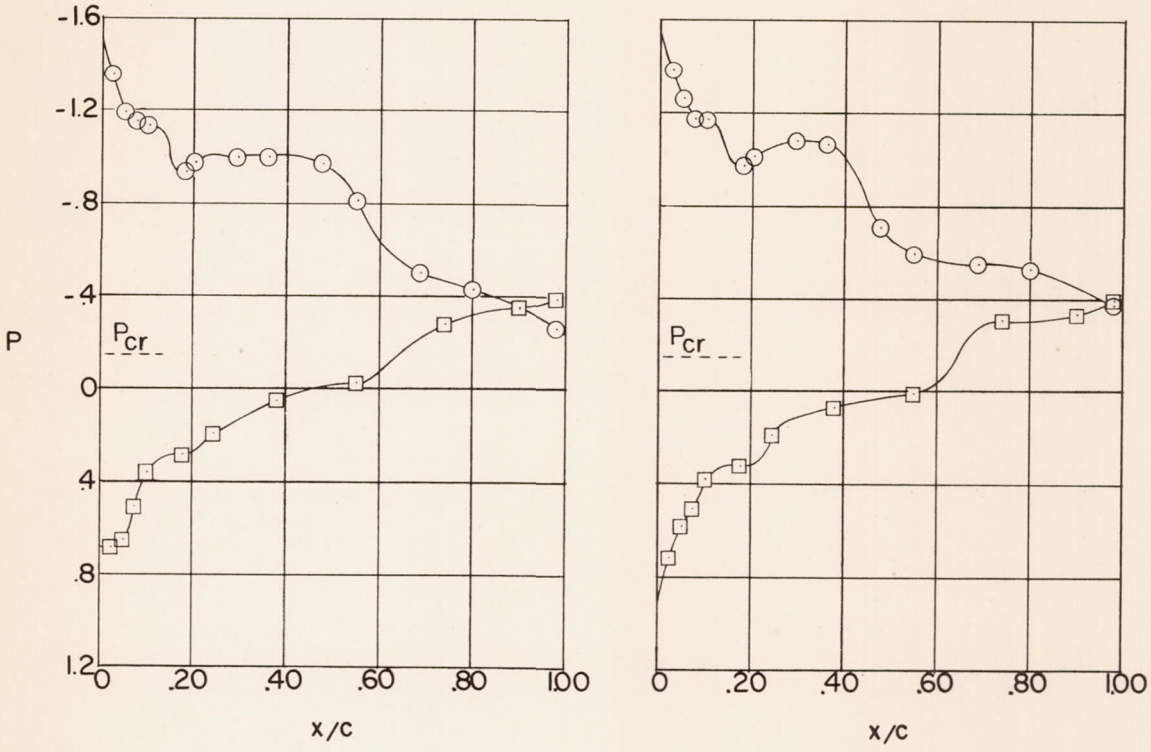

(i) $c_n = 0.80$; $\alpha = 7.3°$.

(j) $c_n = 0.80$; $\alpha = 8.4°$.

Figure 6.- Concluded.

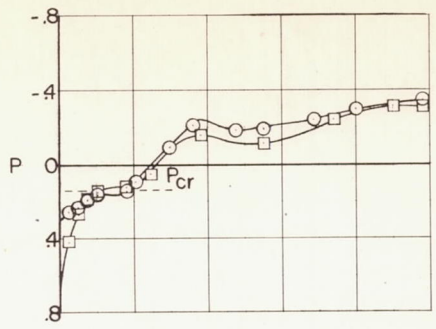

(a) $c_n = 0.05$; $\alpha = 1.5^\circ$.

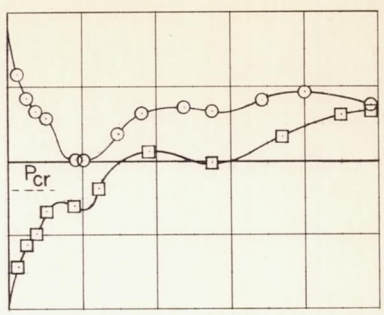

(d) $c_n = 0.28$; $\alpha = 3.3^\circ$.

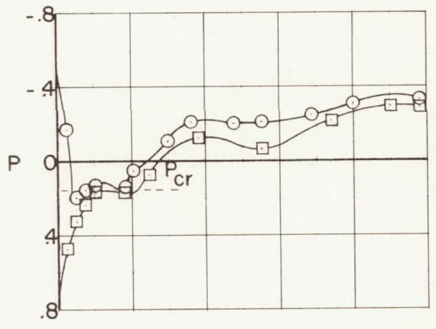

(b) $c_n = 0.10$; $\alpha = 1.8^\circ$.

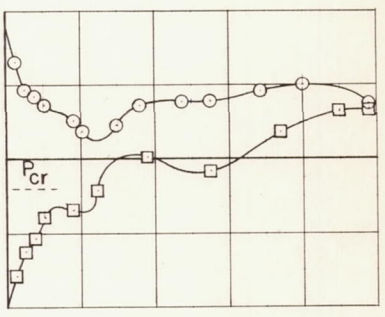

(e) $c_n = 0.35$; $\alpha = 3.6^\circ$.

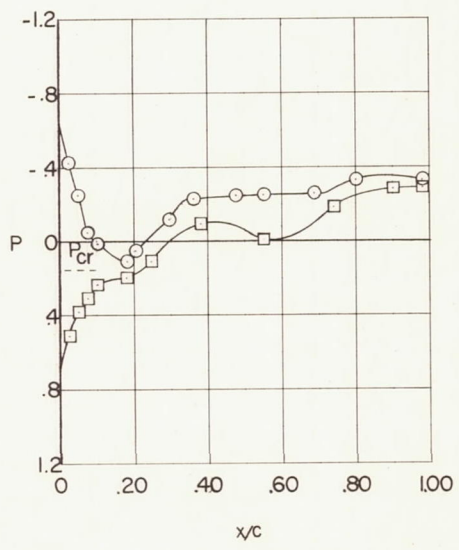

(c) $c_n = 0.19$; $\alpha = 2.6^\circ$.

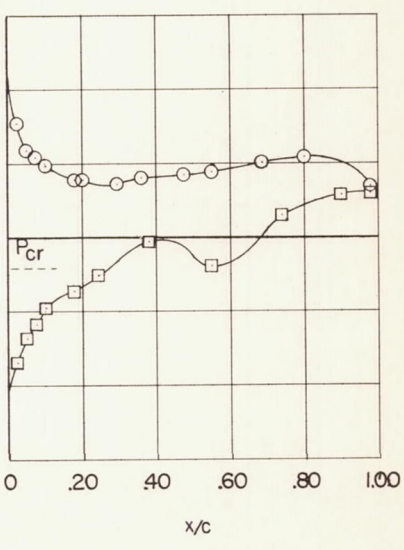

(f) $c_n = 0.46$; $\alpha = 4.6^\circ$.

Figure 7.- Effects of angle of attack on the chordwise pressure distribution of the midsemispan station at a Mach number of 1.10 ± 0.02. X-3 airplane.

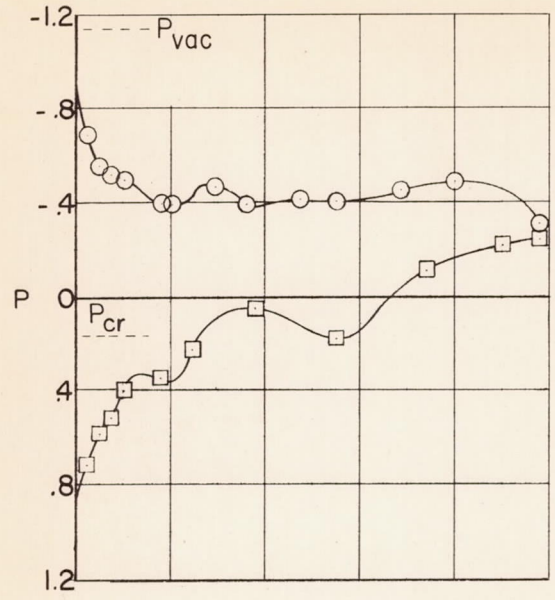

(g) $c_n = 0.55$; $\alpha = 5.7°$.

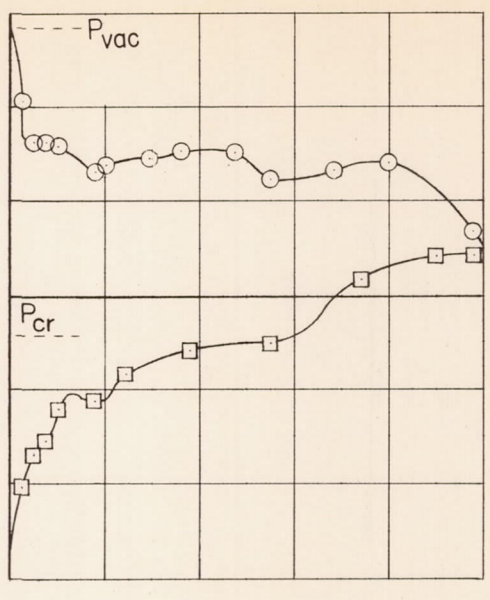

(i) $c_n = 0.73$; $\alpha = 7.4°$.

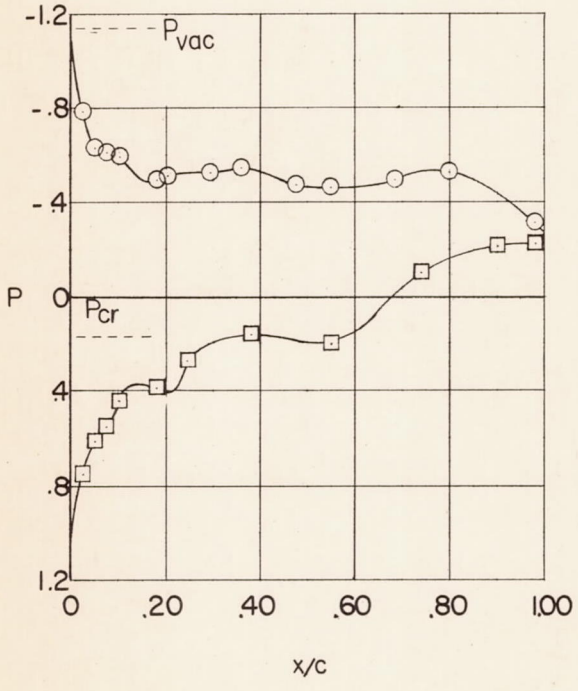

(h) $c_n = 0.64$; $\alpha = 6.8°$.

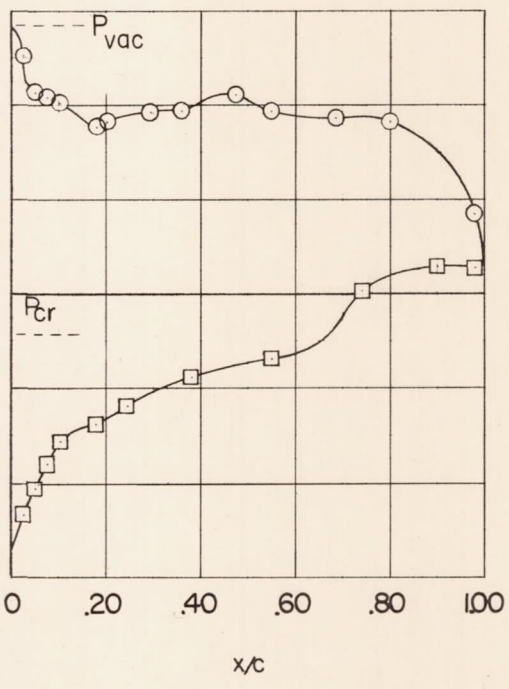

(j) $c_n = 1.02$; $\alpha = 10.6°$.

Figure 7.- Continued.

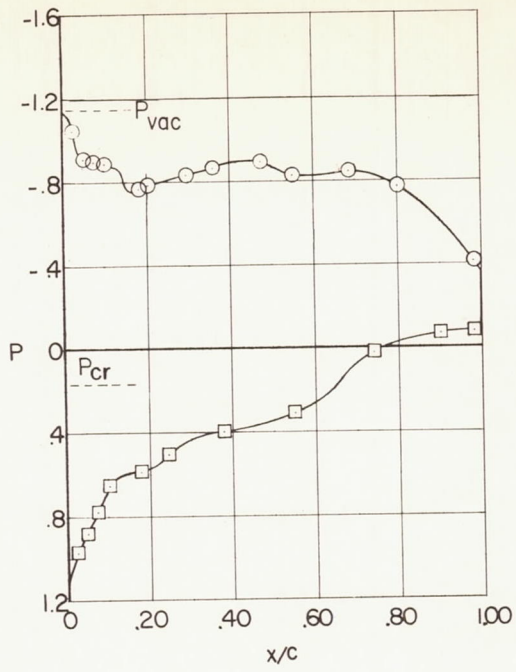

(k) $c_n = 1.13$; $\alpha = 11.8^\circ$.

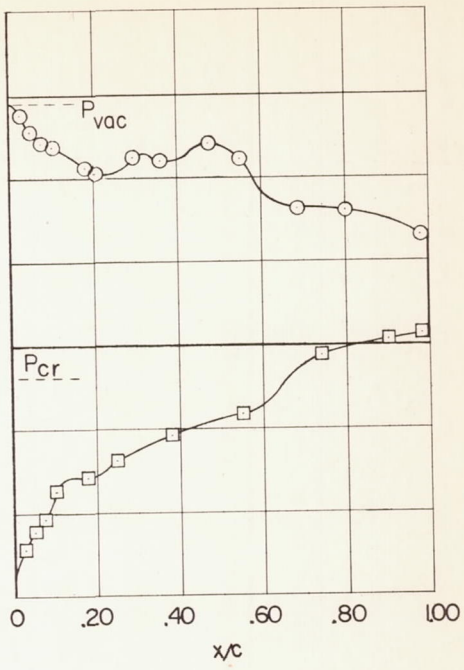

(l) $c_n = 1.15$; $\alpha = 13.1^\circ$.

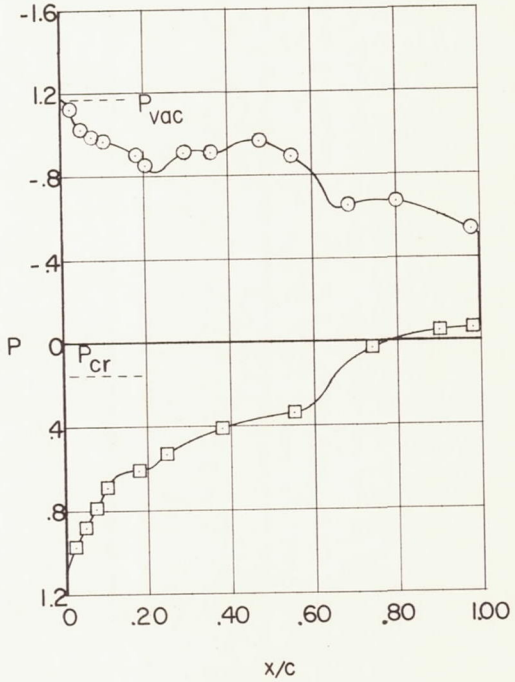

(m) $c_n = 1.15$; $\alpha = 13.4^\circ$.

Figure 7.- Concluded.

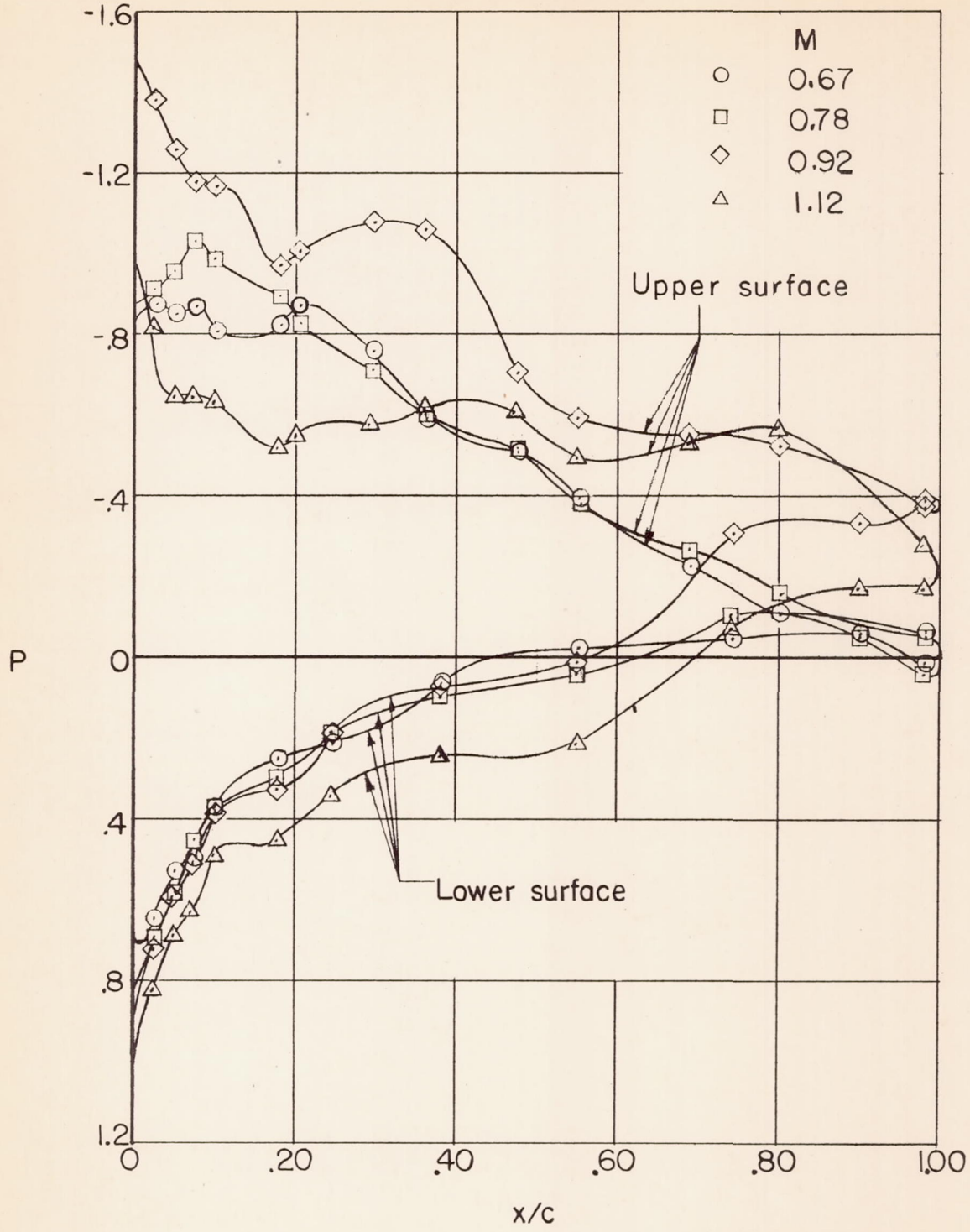

Figure 8.- Effect of Mach number on pressure distribution at midsemispan station at an angle of attack of approximately 8°.

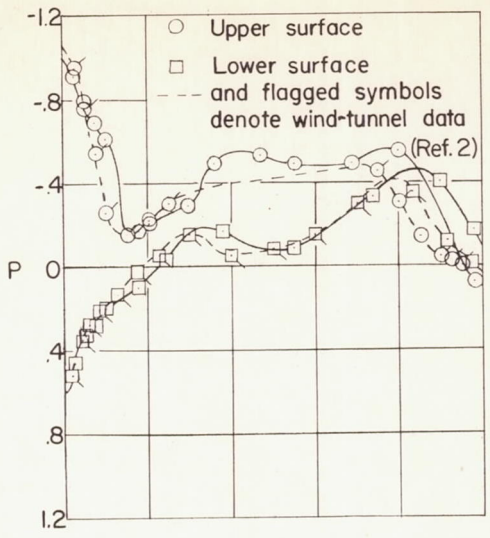

(a) Flight, M = 0.94; wind tunnel, M = 0.92. Flight, $\alpha = 3.4^{\circ}$; wind tunnel, $\alpha = 3.0^{\circ}$.

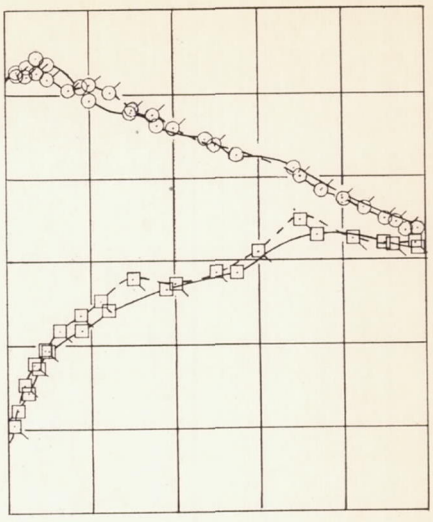

(c) Flight, M = 0.78; wind tunnel, M = 0.80. Flight, $\alpha = 9.2^{\circ}$; wind tunnel, $\alpha = 9.0^{\circ}$.

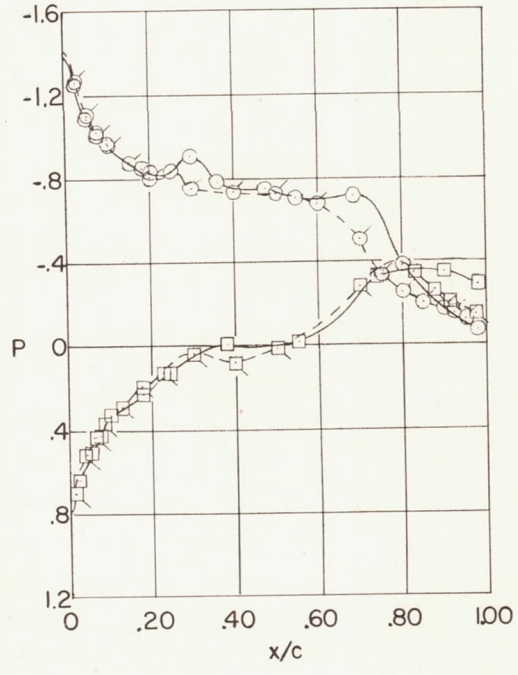

(b) Flight, M = 0.93; wind tunnel, M = 0.90. Flight, $\alpha = 6.2^{\circ}$; wind tunnel, $\alpha = 6.2^{\circ}$.

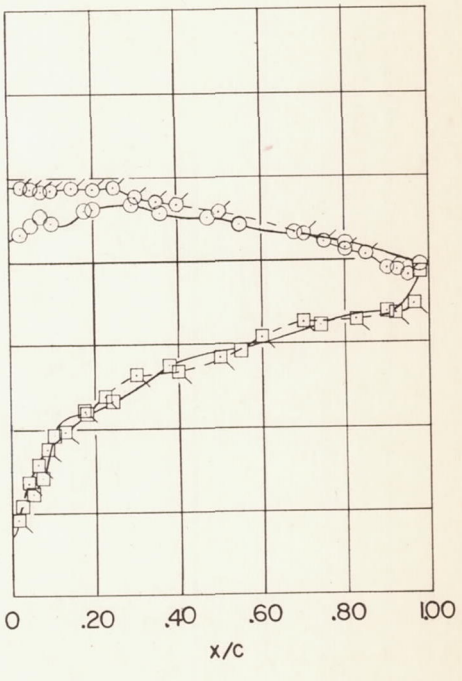

(d) Flight, M = 0.58; wind tunnel, M = 0.60. Flight, $\alpha = 12.7^{\circ}$; wind tunnel, $\alpha = 12.0^{\circ}$.

Figure 9.- Comparison of wind tunnel and flight determined pressure distributions at the midsemispan station. X-3 airplane.

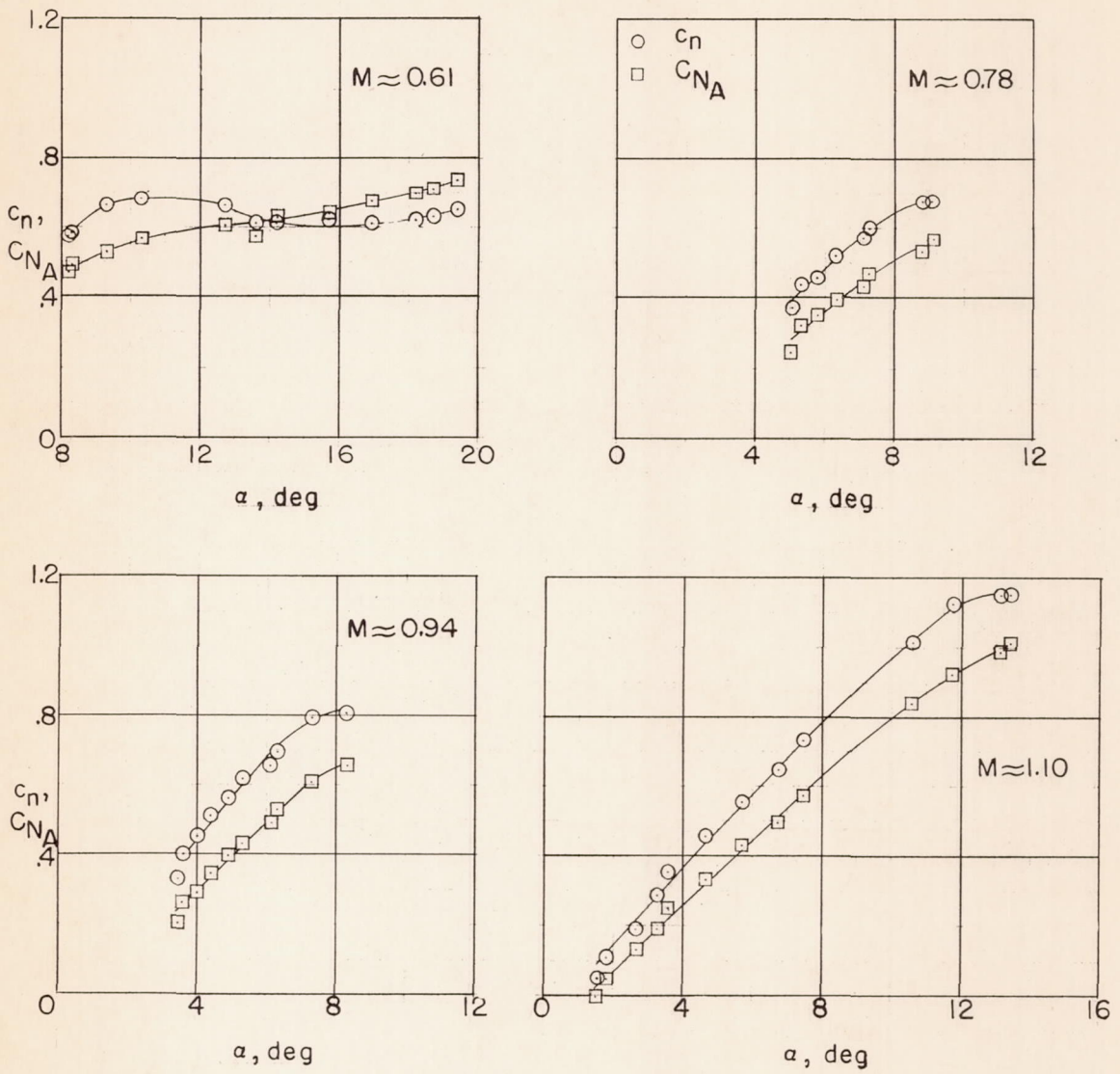

Figure 10.- Variation of airplane and wing midsemispan section normal-force coefficients with angle of attack at various Mach numbers.

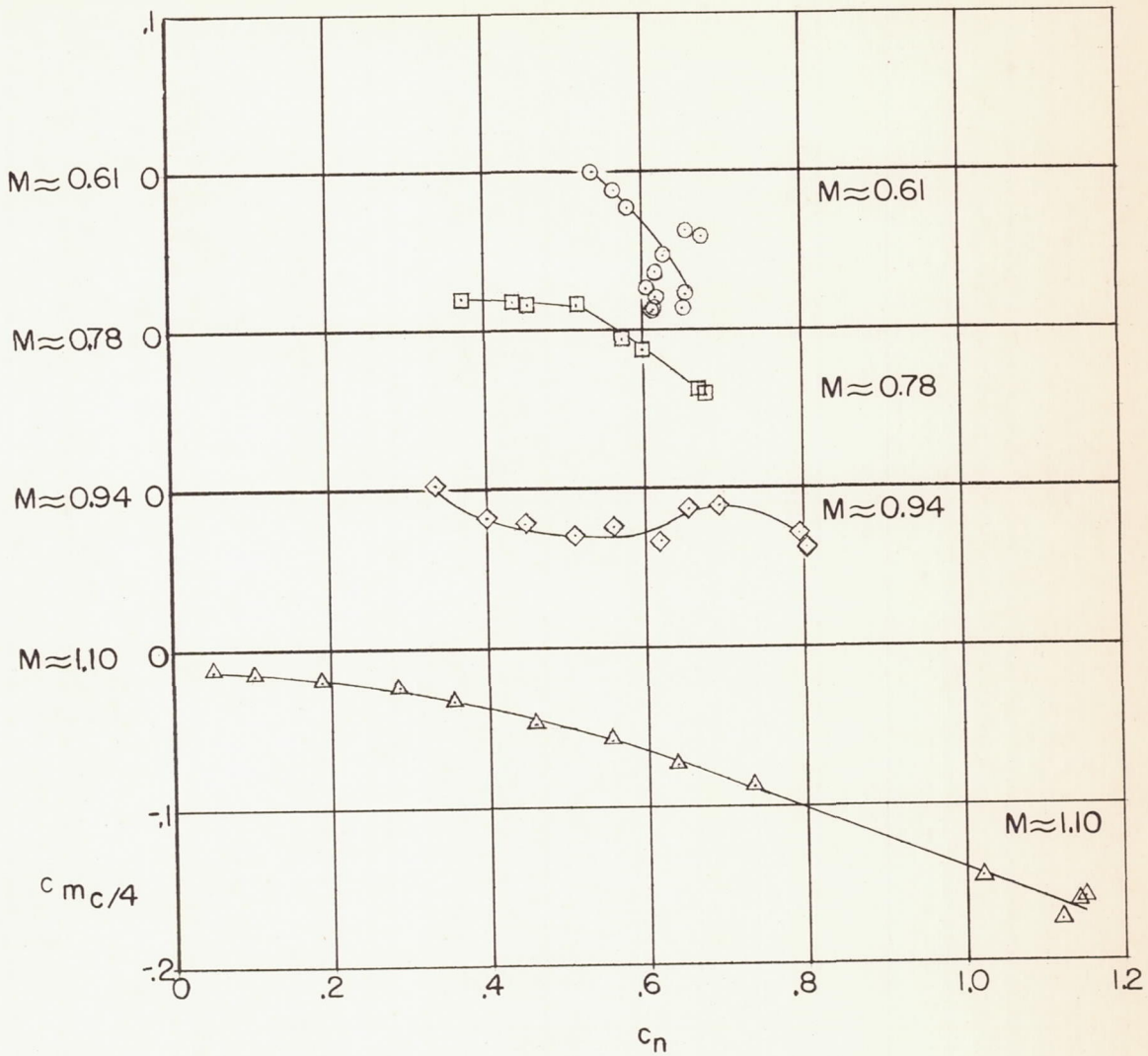

Figure 11.- Variation of section pitching-moment coefficient with section normal-force coefficient at the midsemispan station.

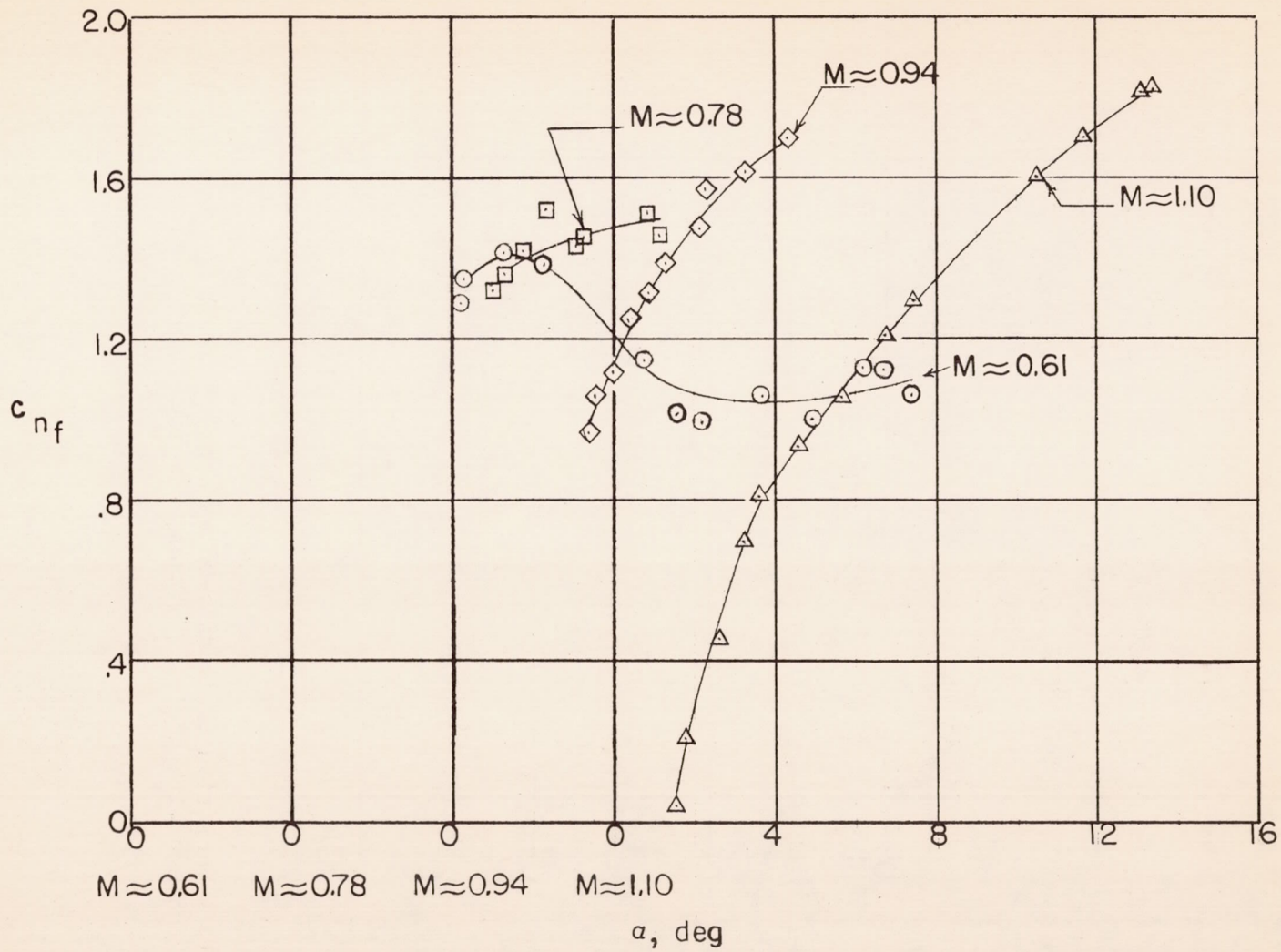

Figure 12.- Variation of leading-edge flap section normal-force coefficient with angle of attack at various Mach numbers.

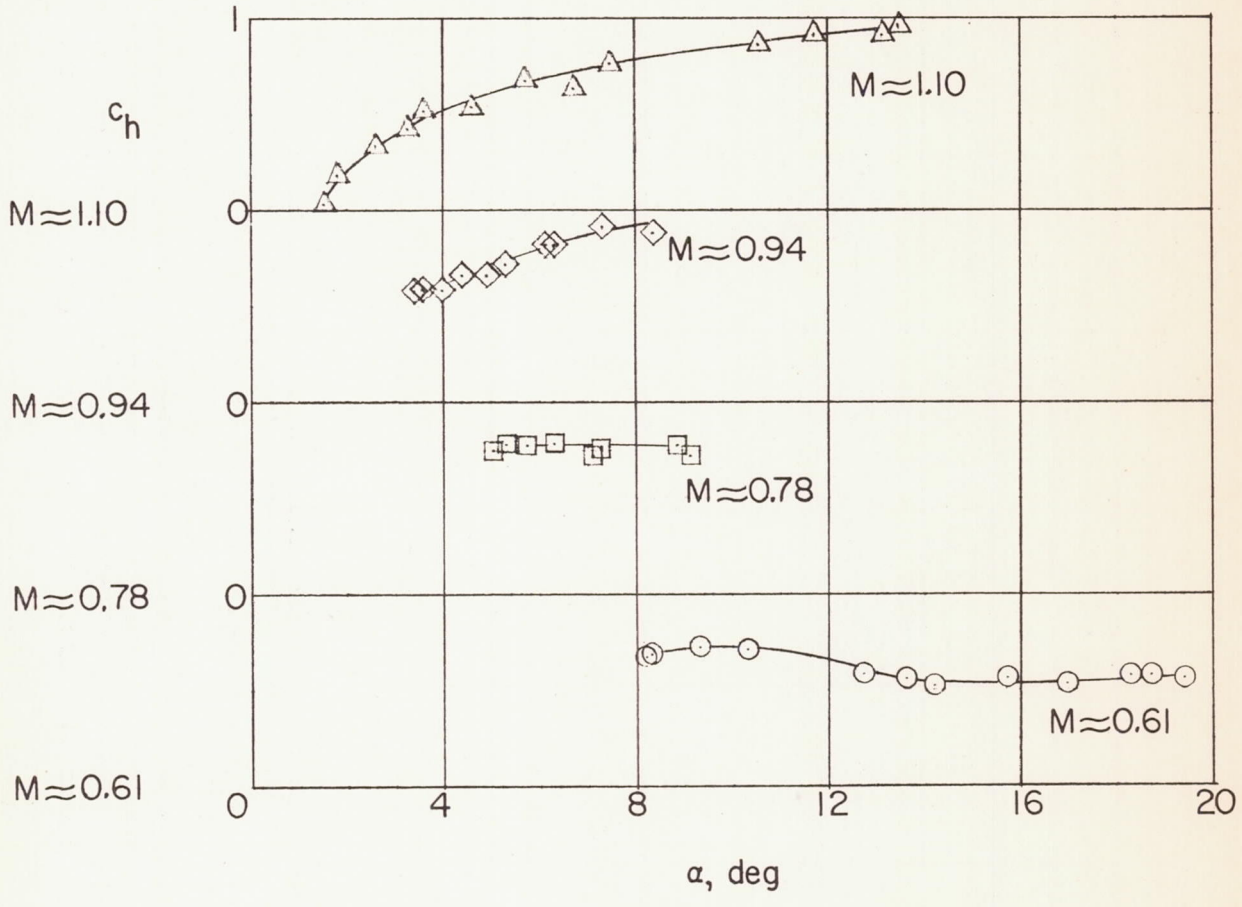

Figure 13.- Variation of leading-edge flap section hinge-moment coefficient with angle of attack at various Mach numbers.

NACA-Langley - 4-7-55 - 350